






Resonant elastic scattering of polarized electrons on H-like ions

D. M. Vasileva ^{1,*}, K. N. Lyashchenko ², A. B. Voitkiv ³, D. Yu. ^{2,4} and O. Yu. Andreev ^{1,5}

¹*Department of Physics, St. Petersburg State University, 7/9 Universitetskaya Naberezhnaya, St. Petersburg 199034, Russia*

²*Institute of Modern Physics, Chinese Academy of Sciences, Lanzhou 730000, China*

³*Institute for Theoretical Physics I, Heinrich-Heine-University of Düsseldorf, Düsseldorf 40225, Germany*

⁴*University of Chinese Academy of Sciences, Beijing 100049, China*

⁵*Petersburg Nuclear Physics Institute named by B.P. Konstantinov of National Research Centre “Kurchatov Institute”, Gatchina, Leningrad District 188300, Russia*



(Received 24 March 2021; revised 11 October 2021; accepted 21 October 2021; published 11 November 2021)

We study the polarization properties of elastic electron scattering on H-like ions using the relativistic QED theory. We calculate the complete set of parameters which describe the scattering of a polarized electron on an initially unpolarized ion and analyze them for both nonresonant and resonant scattering focusing on the LL-shell resonances. The study is carried out for B^{4+} , Ca^{19+} , Kr^{35+} , and Xe^{53+} ions. We demonstrate that for the resonant electron scattering on ions with Z up to 50 both the relativistic spin-orbit and the exchange interaction are equally significant. The possible spin exchange between the incident and bound electrons can fundamentally change the polarization of the scattered electron. We show that the involvement of the autoionizing states leads to quantitative and qualitative changes in the polarization parameters, in particular, to a significant increase in the spin asymmetry.

DOI: [10.1103/PhysRevA.104.052808](https://doi.org/10.1103/PhysRevA.104.052808)

I. INTRODUCTION

The scattering of an unpolarized electron by the Coulomb field of an atomic nucleus has axial symmetry with respect to the direction of the momentum of the incident electron. Mott suggested that in the scattering by the Coulomb field an initially unpolarized electron becomes partially polarized and the resulting polarization is directed perpendicular to the plane of scattering (and therefore changes with the direction of the scattered electron momentum) [1]. It was also noted that if the electron polarized in this way is then scattered on the Coulomb potential again, the differential cross section of this process is no longer symmetric with respect to the direction of the incident electron momentum and therefore the polarization of the electron can be detected experimentally in such scattering. The cause of these effects is most easily seen in the electron rest frame. When the electron is moving in the electric Coulomb field, in the rest frame of the electron there is a magnetic field that interacts with the magnetic moment of the electron. This interaction explains the appearance of asymmetry in the electron scattering.

The Mott prediction was confirmed in a double-scattering experiment in [2]. Since then, the asymmetry arising in Mott scattering has been utilized to produce and measure electron polarization. Today Mott polarimeters are widely used in different fields of physics such as atomic, nuclear, and particle physics [3,4].

A general approach for the description of the electron polarization was initially formulated in [5]. A detailed study of the polarization properties of the Coulomb scattering is

given in [6,7], where the authors proposed to characterize the polarization properties of the scattered electron by three parameters, with the so-called Sherman asymmetry function [8] being of most interest. The Sherman asymmetry function describes both the polarization acquired by the electron during scattering and the possible asymmetry of the differential cross section.

The polarization properties were also studied for electron elastic scattering on neutral atoms. In some of these studies [9–19] the atom was considered as a rigid structure not affected by the collision and therefore representing just an external short-range (electrostatic) potential in which the scattered electron moves. In such an approximation the polarization properties are described by the same three parameters as in the case of the pure Coulomb scattering.

A theory for the description of the polarization properties in electron elastic scattering on one-electron (alkali-metal) atoms, where the bound (valence) electron plays an active role, was presented in [20]. In that paper the parametrization of the polarization properties was generalized to the case of the presence of an active bound electron and in particular the asymmetry function for the resonant elastic electron scattering with the formation of autoionizing states of Cs^- ion was calculated.

The effect of the spin exchange on the polarization properties of an electron elastically scattered on neutral atoms with one valence electron was investigated in [21–27]. There the dependence of the asymmetry in the differential cross section on the initial polarizations of the incident electron and the atom was explored. However, the change in the polarization of the electron and atom after the scattering was not considered.

In this work we study the polarization properties for the elastic electron scattering on highly charged H-like ions.

*Corresponding author: summerdacha64@gmail.com

Compared to the scattering on neutral atoms, this process possesses qualitatively new features caused by the strong and long-range Coulomb field exerted on the electrons by the ionic nucleus. In addition, it is a relatively simple process that can be described within an *ab initio* QED approach which treats, in a natural way, the polarization properties determined by the joint action of the spin-orbit interaction and exchange effects. Since in highly charged ions the interaction of all electrons with the electric field of the atomic nucleus is much stronger than the interelectron interaction, the QED perturbation theory for the interelectron interaction is expected to converge fast.

The elastic electron scattering can proceed via two channels: nonresonant and resonant ones. In the nonresonant channel the electron is scattered on the long-range (Coulomb) potential created by a partially screened nucleus. The resonant channel becomes efficient if the energy of the initial electron configuration is close to the energy of one of the autoionizing states of the corresponding He-like ion.

Then the scattering of an electron can occur due to the formation of a doubly excited state d and its subsequent Auger decay

$$e^- + X^{(Z-1)+}(1s) \rightarrow X^{(Z-2)+}(d) \rightarrow e^- + X^{(Z-1)+}(1s). \quad (1)$$

For the nonresonant region of impact energies the polarization properties are mainly determined by the long-range Coulomb interaction. The formation of intermediate autoionizing states significantly enhances the interelectron interaction and facilitates spin exchange between the electrons that can drastically change the polarization properties of the scattering process. The effect of autoionizing states is stronger than that studied in [20] for the electron scattering on a neutral atom.

We note that the process of the resonant electron scattering on multiply and highly charged ions was experimentally studied in [28–33], where the focus was on measuring differential cross sections. However, the polarization properties of this process were not considered.

The paper is organized as follows. In Sec. II, based on the parametrization proposed in [6,7,20], we introduce the complete set of parameters describing the polarization properties of the scattered electron and perform their calculation within the framework of the QED theory developed in our previous paper [34]. In particular, the calculation takes into account the one- and two-photon exchange corrections, including the Breit interelectron interaction and the retardation effect. Radiation corrections such as the corrections for the electron self-energy and vacuum polarization are taken into account in the first order of the QED perturbation theory. In Sec. III we present numerical results for the polarization parameters in the electron scattering on B^{4+} , Ca^{19+} , Kr^{35+} , and Xe^{53+} ions. Section IV contains a summary and our main conclusions.

II. SCATTERING OF POLARIZED ELECTRONS

In this work we consider the process of scattering in the rest frame of the atomic nucleus which is assumed to be infinitely heavy. Relativistic units are used throughout the paper unless stated otherwise.

A. Scattering theory

The elastic scattering of electrons on H-like ions can proceed via two channels: the Coulomb nonresonant channel and the resonant channel via formation and subsequent decay of intermediate autoionizing states. These two channels are usually described in two different ways. The long-range Coulomb interaction with the nucleus partially screened by the bound electron must be treated nonperturbatively. In contrast, in the resonant channel, the formation of the autoionizing states is described within QED, which implies the use of the QED perturbation theory. Nevertheless, in order to correctly account for the interference between the two channels, the whole process must be described within a single approach. For this purpose, we use a method we developed in [34]. Below we present the key points of our approach.

We introduce $\Psi_{m_i, \mu_i}^i(\mathbf{p}_i)$ and $\Psi_{m_f, \mu_f}^f(\mathbf{p}_f)$ describing the initial and final states of the two-electron system

$$\Psi_{m_i, \mu_i}^i(\mathbf{p}_i) = \frac{1}{\sqrt{2}} \det \{ \psi_{p_i, \mu_i}^{(+)}(\mathbf{r}_1) \psi_{1s, m_i}(\mathbf{r}_2) \}, \quad (2)$$

$$\Psi_{m_f, \mu_f}^f(\mathbf{p}_f) = \frac{1}{\sqrt{2}} \det \{ \psi_{p_f, \mu_f}^{(-)}(\mathbf{r}_1) \psi_{1s, m_f}(\mathbf{r}_2) \}, \quad (3)$$

where m_i and m_f are the bound (1s) electron total momentum projections on the z axis and $\psi_{p, \mu}^{(\pm)}(\mathbf{r})$ is the incoming (+) or outgoing (−) wave function of an electron in an external Coulomb field with the asymptotic momentum ($\mathbf{p} = p\hat{\mathbf{v}}$)

$$\psi_{p, \mu}^{(\pm)}(\mathbf{r}) = N \sum_{jlm} \Omega_{jlm}^{+}(\mathbf{v}) v_{\mu} e^{\pm i\phi_{jl}} i^l \psi_{\varepsilon jlm}(\mathbf{r}), \quad (4)$$

where

$$N = \frac{(2\pi)^{3/2}}{\sqrt{p\varepsilon}} \quad (5)$$

is the normalization factor, ϕ_{jl} is the phase shift [35], and the spinor v_{μ} describes the electron with the (asymptotic) projection of spin μ on the direction $\hat{\boldsymbol{\zeta}} = \boldsymbol{\zeta}/|\boldsymbol{\zeta}|$ and is determined by the equation

$$\frac{1}{2}(\hat{\boldsymbol{\zeta}}\boldsymbol{\sigma})v_{\mu} = \mu v_{\mu}. \quad (6)$$

The Coulomb scattering amplitude is well known [7,8]. In our previous work we showed that the Coulomb amplitude can be expressed as

$$U_{\mu_i \mu_f}^{\text{Coul}} = N^2 \frac{(-1)^p}{(2\pi)^2} \sum_m [v_{\mu_f}(\mathbf{v}_f)]_m^* \mathcal{M}_{m \mu_i}^{\text{Coul}}(\theta, \varphi). \quad (7)$$

Following [36], we introduced the matrix \mathcal{M} as

$$\mathcal{M}^{\text{Coul}}(\theta, \varphi) = \begin{pmatrix} f(\theta) & g(\theta)e^{-i\varphi} \\ -g(\theta)e^{i\varphi} & f(\theta) \end{pmatrix}, \quad (8)$$

where $f(\theta)$ and $g(\theta)$ are the relativistic scattering amplitudes

$$f(\theta) = \frac{1}{2\pi i} \sum_{jl} |\varkappa| (e^{2i\phi_{\varkappa}} - 1) P_l^0(\cos \theta), \quad (9)$$

$$g(\theta) = \frac{1}{2\pi i} \sum_l (e^{2i\phi_{\varkappa=-l-1}} - e^{2i\phi_{\varkappa=l}}) P_l^1(\cos \theta), \quad (10)$$

where $\varkappa = (j + \frac{1}{2})(-1)^{j+l+1/2}$ is the Dirac quantum number, $\phi_{\varkappa} \equiv \phi_{jl}$, and P_l^m are the associated Legendre polynomials.

In order to describe the electron scattering process within the QED perturbation theory, we introduce the formal perturbation series for the Coulomb interaction of the incident electron with the screened nucleus:

$$U_{\text{pert}} = \sum_k (U_k^{\text{Coul}} + U_k^{\text{Auger}}). \quad (11)$$

Here k denotes the order of the QED perturbation series. The purpose of this expansion is to establish the phase difference between the Coulomb amplitude obtained nonperturbatively [see Eq. (7)] and the Coulomb amplitude obtained as a formal series within the QED perturbation theory $U_{\text{pert}}^{\text{Coul}} = \sum_k U_k^{\text{Coul}}$. Then the formal series for the Coulomb amplitude $U_{\text{pert}}^{\text{Coul}}$ can be replaced by U^{Coul} with the corresponding phase factor. Within our method, we define the amplitudes so that the phase factor is equal to unity:

$$U_{\text{pert}}^{\text{Coul}} = U^{\text{Coul}}. \quad (12)$$

Below we assume that Eq. (12) takes place. Accordingly, the amplitude can be presented as

$$U = U^{\text{Coul}} + U^{\text{Auger}}. \quad (13)$$

The amplitude $U^{\text{Auger}} = \sum_k U_k^{\text{Auger}}$ is calculated within the QED perturbation theory [34].

Within the standard QED perturbation theory, the Furry picture is employed where the interaction of all electrons with the Coulomb field of the nucleus ($V = -\alpha Z/r$) is fully taken into account from the onset. However, in our previous work we demonstrated that, in the case of electron scattering on an ion that has bound electrons, the terms of the perturbation series for the resonant amplitude (U) would be divergent. These divergences arise because the long-range Coulomb interaction between the incident and bound electrons is described with a finite number of perturbation series terms. This problem was discussed in detail in [34]. We can circumvent this issue by considering the incident electron as moving in the field $V = -\alpha(Z - 1)/r$ with the corresponding modification of the

Furry picture. Thus, the long-range interaction of the incident electron with the bound electron is included in the Coulomb amplitude U^{Coul} . The interaction of the incident electron with the remaining potential $V = \alpha/r$ is taken into account within the perturbation theory. The divergences in these additional terms completely cancel the divergences arising in the perturbation series for U^{Auger} .

For the resonant part of the amplitude we employ the line-profile approach (LPA) [37]. Within the LPA the energy level of an atomic system is associated with a resonance in some scattering process. Usually, the photon (ω) scattering is considered. The amplitude of this process is connected with the S matrix as

$$S = (-2\pi i)\delta(E_i - E_f)U. \quad (14)$$

In [37] we showed that it can be expressed as

$$U_{A_0} = T^+ \frac{1}{\omega + E_{A_0} - V} T, \quad (15)$$

where T and T^+ describe the absorption and emission of the photon (ω) and E_{A_0} is the energy of the ground state. The matrix V can be presented as

$$V = V^{(0)} + \Delta V, \quad (16)$$

where $V^{(0)}$ is the sum of one-electron Dirac Hamiltonians and represents the noninteracting (with the quantized fields) electrons and ΔV includes various QED corrections and is derived order by order within the QED perturbation theory. The excited states are associated with the corresponding resonances defined by Eq. (15).

A detailed description of this method and the derivation of the matrix V were given in [37]. Below we present the most important corrections for the process under consideration. We note that in this work the spin of the nucleus is neglected.

First we discuss the interelectron interaction corrections. The photon propagator in the Coulomb gauge reads

$$D_{\mu_1\mu_2}^{c,t}(x_1, x_2) = \int_{-\infty}^{\infty} d\Omega I_{\mu_1\mu_2}^{c,t}(|\Omega|, r_{12}) e^{-i\Omega(t_1 - t_2)}, \quad (17)$$

where $r_{12} = |\mathbf{r}_1 - \mathbf{r}_2|$ and

$$I_{\mu_1\mu_2}^c = \frac{\delta_{\mu_1 0} \delta_{\mu_2 0}}{r_{12}}, \quad (18)$$

$$I_{\mu_1\mu_2}^t(\Omega) = -\left(\frac{\delta_{\mu_1\mu_2}}{r_{12}} e^{i\Omega r_{12}} + \frac{\partial}{\partial x_1^{\mu_1}} \frac{\partial}{\partial x_2^{\mu_2}} \frac{1 - e^{i\Omega r_{12}}}{r_{12}\Omega^2} \right) (1 - \delta_{\mu_1 0})(1 - \delta_{\mu_2 0}). \quad (19)$$

Here $I_{\mu_1\mu_2}^c$ describes the Coulomb photons and $I_{\mu_1\mu_2}^t$ corresponds to the Breit interaction.

The one-photon exchange correction can be written in the form

$$\Delta V^{1\text{ph}} \equiv \alpha I(| - \varepsilon_a + \varepsilon_{a'} |)_{a'b'ab} \quad (20)$$

$$= \alpha \int d\mathbf{r}_1 d\mathbf{r}_2 \bar{\psi}_{a'}(\mathbf{r}_1) \bar{\psi}_{b'}(\mathbf{r}_2) \gamma_1^{\mu_1} \gamma_2^{\mu_2} I_{\mu_1\mu_2}(| - \varepsilon_a + \varepsilon_{a'} |, r_{12}) \psi_a(\mathbf{r}_1) \psi_b(\mathbf{r}_2). \quad (21)$$

The two-photon exchange correction reads

$$\Delta V^{2\text{ph}}(\omega) = \alpha^2 \frac{i}{2\pi} \sum_{n_1 n_2}^{E_{n_1 n_2}^{(0)} \neq E_{ab}^{(0)}} \int_{-\infty}^{\infty} d\Omega \frac{I(|\Omega|)_{a'b'n_1 n_2} I(| - \Omega - \varepsilon_a + \varepsilon_{a'} |)_{n_1 n_2 ab}}{[-\Omega + \varepsilon_{a'} - \varepsilon_{n_1}(1 - i0)][E_{A_0} + \omega + \Omega - \varepsilon_{a'} - \varepsilon_{n_2}(1 - i0)]} \quad (22)$$

$$-\alpha^2 \frac{i}{2\pi} \sum_{n_1 n_2}^{E_{n_1 n_2}^{(0)} = E_{ab}^{(0)}} \int_{-\infty}^{\infty} d\Omega \frac{I(|\Omega|)_{a'b'n_1 n_2} I(|-\Omega - \varepsilon_a + \varepsilon_{a'}|)_{n_1 n_2 ab}}{(\Omega - \varepsilon_{a'} + \varepsilon_{n_1} + \varepsilon_{n_2} i0)[E_{A_0} + \omega + \Omega - \varepsilon_{a'} - \varepsilon_{n_2}(1 - i0)]}, \quad (23)$$

where $E_{n_1 n_2}^{(0)} = \varepsilon_{n_1} + \varepsilon_{n_2}$ and $E_{ab}^{(0)} = \varepsilon_a + \varepsilon_b$ are the sums of one-electron Dirac energies.

For the systems under consideration ($Z < 54$) the so-called Breit approximation can be employed. In this approximation we disregard the retardation:

$$I_{\mu_1 \mu_2}^t(\Omega) = I_{\mu_1 \mu_2}^t(0). \quad (24)$$

Then the two-photon exchange correction becomes

$$\Delta V^{2\text{ph}}(\omega) = \alpha^2 \sum_{n_1 n_2}^{E_{n_1 n_2}^{(0)} \neq E_{ab}^{(0)}} \frac{(\Lambda_{n_1}^{(+)} \Lambda_{n_2}^{(+)} - \Lambda_{n_1}^{(-)} \Lambda_{n_2}^{(-)}) I_{a'b'n_1 n_2}(0) I_{n_1 n_2 ab}(0)}{E_{A_0} + \omega - \varepsilon_{n_1} - \varepsilon_{n_2}}, \quad (25)$$

where $\Lambda_n^{(\pm)}$ are the projectors on the states with positive (negative) energies. The resonance condition for Eq. (15) in the lowest order of QED perturbation theory is given by

$$\omega + E_{A_0} = \varepsilon_a + \varepsilon_b. \quad (26)$$

Other important corrections are the radiative corrections [37,38]: the electron self-energy and the vacuum polarization. The real part of the radiative corrections is subject to renormalization. It contributes mainly to the energy of the two-electron configurations or to the positions of the resonances. Taking into account the real part of the self-energy corrections leads to various shifts of the resonances. The imaginary part is convergent and usually gives the leading contribution to the width of the energy level. Two-photon exchange corrections can also give an important contribution to the width.

Below we demonstrate that the polarization properties are affected by the presence of the resonances. Accordingly, the influence of the radiative corrections on the polarization properties is determined by their contributions to the positions and widths of the resonances. For the calculation of the electron self-energy correction, we use the methods presented in [38–41].

The matrix V is a complex symmetric matrix. The eigenvalues of the matrix V can be written as $E - i/2\Gamma$, where E is the energy of a state of the system and Γ is the width of the energy level.

We consider V as a block matrix:

$$V = \begin{bmatrix} V_{11} & V_{12} \\ V_{21} & V_{22} \end{bmatrix} = \begin{bmatrix} V_{11}^{(0)} + \Delta V_{11} & \Delta V_{12} \\ \Delta V_{21} & V_{22}^{(0)} + \Delta V_{22} \end{bmatrix}. \quad (27)$$

The matrix V_{11} is defined on the set g . In this case, we choose the set g to contain all two-electron configurations formed using the bound electron states with the principal quantum numbers $n = 1, 2, 3$ and continuum state describing the incident electron. The treatment of the continuum electron is discussed in detail in [42]. The matrix V_{11} is a finite matrix and can be diagonalized numerically:

$$V_{11}^{\text{diag}} = B^t V_{11} B, \quad B^t B = I. \quad (28)$$

Using the matrix B , we obtain the expression for the eigenvectors of V ,

$$\Phi_{n_g} = \sum_{k_g \in g} B_{k_g n_g} \Psi_{k_g}^{(0)} + \sum_{k \notin g, l_g \in g} [\Delta V_{21}]_{kl_g} \frac{B_{l_g n_g}}{E_{n_g}^{(0)} - E_k^{(0)}} \Psi_k^{(0)} + \dots, \quad (29)$$

where n_g describes the reference state. The indices k and l_g denote the two-electron configurations: The index l_g runs over all configurations of the set g ; the index k runs over all configurations not included in the set g . The amplitude U^{Auger} can then be expressed as a matrix element of the operator $\Delta \hat{V}$,

$$U^{\text{Auger}} = \langle \Psi_{m_f, \mu_f}^f(\mathbf{p}_f) | \Delta \hat{V} | \Phi_{\text{ini}} \rangle, \quad (30)$$

where $\Psi_{m_f, \mu_f}^f(\mathbf{p}_f)$ describes the final state of the scattering system [see Eq. (3)] and Φ_{ini} is given by Eq. (29) with the initial state of the system taken as the reference state.

B. Polarization theory

A partially polarized electron beam is described by the density matrix $\hat{\rho}_s$ [35,43],

$$\hat{\rho}_s = \frac{1}{2}(m + \hat{p})(1 - \gamma_5 \hat{s}), \quad (31)$$

where

$$\hat{p} = p_\mu \gamma^\mu = p_0 \gamma_0 - \mathbf{p} \boldsymbol{\gamma}, \quad (32)$$

$$\hat{s} = s_\mu \gamma^\mu = s_0 \gamma_0 - \mathbf{s} \boldsymbol{\gamma}, \quad (33)$$

$$\mathbf{s} = \boldsymbol{\zeta} + \frac{(\boldsymbol{\zeta} \mathbf{p}) \mathbf{p}}{m(\varepsilon + m)}, \quad s_0 = \frac{\boldsymbol{\zeta} \mathbf{p}}{m}, \quad (34)$$

m is the electron mass, $\boldsymbol{\zeta}$ is the polarization vector of the electron in the electron rest frame, and $P = |\boldsymbol{\zeta}| \leq 1$ is the degree of polarization. Dirac gamma matrices here are defined as

$$\gamma_0 = \beta = \begin{pmatrix} I & 0 \\ 0 & -I \end{pmatrix}, \quad (35)$$

$$\boldsymbol{\gamma} = \beta \boldsymbol{\alpha} = \begin{pmatrix} 0 & \boldsymbol{\sigma} \\ -\boldsymbol{\sigma} & 0 \end{pmatrix}, \quad (36)$$

$$\gamma_5 = i\gamma_1 \gamma_2 \gamma_3 \gamma_0. \quad (37)$$

If the density matrix of the initial state is $\hat{\rho}_i$, then the density matrix describing the electron after scattering can be written as

$$\hat{\rho} = S\hat{\rho}_i\bar{S}, \quad (38)$$

where S is the S matrix $\bar{S} = \gamma_0 S^\dagger \gamma_0$.

If one is interested in the probability of transition from state i described by the density matrix $\hat{\rho}_i$ into state f described by $\hat{\rho}_f$, one should use the following formula for the differential cross section with the appropriate coefficient [5]:

$$d\sigma(\mathbf{p}_i, \boldsymbol{\zeta}_i; \mathbf{p}_f, \boldsymbol{\zeta}_f) \sim \text{Tr}(\hat{\rho}_f \hat{\rho}) = \text{Tr}(\hat{\rho}_f S \hat{\rho}_i \bar{S}). \quad (39)$$

We note that here $\hat{\rho}_f$ is the density matrix that determines the state of the electron detected in the experiment rather than the state of the scattered electron.

In the process under consideration the initial and final electron states are positive energy states. In this case, taking into account that the electron wave function can be written in terms of two-electron wave functions with two certain polarizations, the density matrix can be represented by a 2×2 matrix [5,35]. This matrix can be written as

$$\rho_\zeta = \frac{1}{2}(1 + \boldsymbol{\zeta}\boldsymbol{\sigma}), \quad (40)$$

where $\boldsymbol{\zeta}$ is the polarization vector of the electron in the electron rest frame. The density matrix with $|\boldsymbol{\zeta}| = 1$ describes a pure state with certain polarization. For mixed states $|\boldsymbol{\zeta}| < 1$. A completely unpolarized state corresponds to $\boldsymbol{\zeta} = 0$.

In the case of the elastic electron scattering on a hydrogenlike ion we must handle the two-electron system. Since in the initial state the polarizations of the incident and bound electrons are assumed to be independent, the density matrix of the initial two-electron state can be taken as a direct product of the corresponding single-electron density matrices [5]. Accordingly, in order to describe the initial state of the scattering system, we use the 4×4 density matrices of the form

$$\hat{\rho}_{\zeta\eta} = \frac{1}{4}(1 + \boldsymbol{\zeta}\boldsymbol{\sigma}_1)(1 + \boldsymbol{\eta}\boldsymbol{\sigma}_2), \quad (41)$$

where $\boldsymbol{\zeta}$ is the polarization vector of the incident (or scattered) electron and $\boldsymbol{\eta}$ is the polarization vector of the ion (in our case, the polarization of the $1s$ electron). The matrix indices 1 and 2 refer to the incident (scattered) and $1s$ electrons, respectively.

It is convenient to take the z axis in the direction of the incident beam and introduce angles θ and φ for the direction of the scattered electron momentum. The scattering is described by the 4×4 matrix M [20]. Using our method (see Sec. II A), we can express the elements of matrix M via the amplitude defined by Eq. (13):

$$\begin{aligned} M_{m_i, \mu_i; m_f, \mu_f}(\theta, \varphi) &= U_{m_i, \mu_i; m_f, \mu_f}(\theta, \varphi) \\ &= U_{\mu_i \mu_f}^{\text{Coul}}(\theta, \varphi) \delta_{m_i m_f} + U_{m_i, \mu_i; m_f, \mu_f}^{\text{Auger}}(\theta, \varphi). \end{aligned} \quad (42)$$

We note that in the calculation of the amplitude all spin projections must be taken with respect to one chosen axis (we use the z axis).

It is convenient to consider the total amplitude of the process as the sum of the Coulomb amplitude corresponding to the Coulomb scattering by the screened potential of the nucleus $(Z - 1)/r$ and the Auger amplitude. The Auger

amplitude includes contributions from the interelectron interaction: the resonant channel as well as the remaining part of the nonresonant channel.

The scattering matrix M can be expressed in terms of Pauli matrices $\hat{\sigma}$. Since the matrix M must be invariant with respect to the space rotation and reflection and also time reversal, only the following six linearly independent terms remain [20]:

$$\begin{aligned} M &= a_0 + a_1(\boldsymbol{\sigma}_1 \hat{\mathbf{n}}) + a_2(\boldsymbol{\sigma}_2 \hat{\mathbf{n}}) + a_{12}(\boldsymbol{\sigma}_1 \hat{\mathbf{n}})(\boldsymbol{\sigma}_2 \hat{\mathbf{n}}) \\ &\quad + b_{12}(\boldsymbol{\sigma}_1 \hat{\mathbf{k}})(\boldsymbol{\sigma}_2 \hat{\mathbf{k}}) + c_{12}(\boldsymbol{\sigma}_1 \hat{\mathbf{q}})(\boldsymbol{\sigma}_2 \hat{\mathbf{q}}). \end{aligned} \quad (43)$$

Here the vectors $\hat{\mathbf{n}}$, $\hat{\mathbf{k}}$, and $\hat{\mathbf{q}}$ are introduced,

$$\hat{\mathbf{n}} = \frac{\mathbf{p}_i \times \mathbf{p}_f}{|\mathbf{p}_i \times \mathbf{p}_f|}, \quad (44)$$

$$\hat{\mathbf{k}} = \frac{\mathbf{p}_i + \mathbf{p}_f}{|\mathbf{p}_i + \mathbf{p}_f|}, \quad (45)$$

$$\hat{\mathbf{q}} = \frac{\mathbf{p}_i - \mathbf{p}_f}{|\mathbf{p}_i - \mathbf{p}_f|}, \quad (46)$$

and a_0 , a_1 , a_2 , a_{12} , b_{12} , and c_{12} are functions of only θ . These coefficients can be easily obtained if the elements of the matrix M are known (for details see Appendix A). For the Coulomb scattering of an electron, M reduces to

$$M^{\text{Coul}} = \mathcal{M}^{\text{Coul}}(\theta, \varphi) \otimes I = f(\theta) + ig(\theta)(\boldsymbol{\sigma}_1 \hat{\mathbf{n}}), \quad (47)$$

where I is the 2×2 identity matrix and $\mathcal{M}^{\text{Coul}}(\theta, \varphi)$ is a matrix defined by Eq. (8). We note that the scattering can be fully described with 11 real numbers since the matrix M is determined by six complex numbers [Eq. (43)] and the phase of M can be chosen arbitrarily [20].

If the initial state is described by some density matrix $\hat{\rho}_i$, the density matrix of the two-electron system after the scattering is given by

$$\hat{\rho} = M \hat{\rho}_i M^\dagger \quad (48)$$

and the scattered electron polarization can be obtained using

$$\boldsymbol{\zeta}^e = \frac{\text{Tr}(\hat{\rho} \boldsymbol{\sigma}_1)}{\text{Tr}(\hat{\rho})}. \quad (49)$$

The expression for the differential cross section is determined by the experimental setup. We suppose that the properties of the electrons that are detected in the experiment are described by the density matrix $\hat{\rho}_f$. Then the corresponding differential cross section can be obtained with the use of the formula

$$\begin{aligned} d\sigma(\mathbf{p}_i, \boldsymbol{\zeta}_i; \mathbf{p}_f, \boldsymbol{\zeta}_f, \boldsymbol{\eta}_f) \\ = \frac{2\pi}{j} \text{Tr}(\hat{\rho}_f M \hat{\rho}_i M^\dagger) \delta(\varepsilon_f - \varepsilon_i) \frac{d^3 \mathbf{p}_f}{(2\pi)^3}, \end{aligned} \quad (50)$$

$$j = \frac{p_i}{\varepsilon_i}, \quad (51)$$

$$\hat{\rho}_i = \frac{1}{4}(1 + \boldsymbol{\zeta}_i \boldsymbol{\sigma}_1)(1 + \boldsymbol{\eta}_i \boldsymbol{\sigma}_2), \quad (52)$$

$$\hat{\rho}_f = \frac{1}{4}(1 + \boldsymbol{\zeta}_f \boldsymbol{\sigma}_1)(1 + \boldsymbol{\eta}_f \boldsymbol{\sigma}_2). \quad (53)$$

The matrix $\hat{\rho}_i$ taken in the form (52) describes the initial state, where $\boldsymbol{\zeta}_i$ and $\boldsymbol{\eta}_i$ are the polarizations of the incident and bound electrons, respectively.

If an electron is scattered from an unpolarized ion and only the electron polarization is of interest, in order to obtain the

respective differential cross section one should set η_i and η_f in Eqs. (50)–(53) to zero. After calculating the trace in Eq. (50) we get the formula

$$\begin{aligned} \frac{d\sigma}{d\Omega}(\mathbf{p}_i, \zeta_i; \mathbf{p}_f, \zeta_f) &= \frac{1}{4} w \{ I(\theta)(1 + \zeta_i \zeta_f) + D(\theta)(\zeta_i \hat{\mathbf{n}} + \zeta_f \hat{\mathbf{n}}) \\ &\quad + F(\theta)[\zeta_i \times \zeta_f] \hat{\mathbf{n}} - G(\theta)[\zeta_i \times \hat{\mathbf{n}}][\zeta_f \times \hat{\mathbf{n}}] \\ &\quad - H(\theta)[\zeta_i \times \hat{\mathbf{k}}][\zeta_f \times \hat{\mathbf{k}}] - K(\theta)[\zeta_i \times \hat{\mathbf{q}}][\zeta_f \times \hat{\mathbf{q}}] \}, \end{aligned} \quad (54)$$

where

$$I(\theta) = |a_0|^2 + |a_1|^2 + |a_2|^2 + |a_{12}|^2 + |b_{12}|^2 + |c_{12}|^2, \quad (55)$$

$$D(\theta) = 2 \operatorname{Re}(a_0 a_1^* + a_2 a_{12}^*), \quad (56)$$

$$F(\theta) = 2 \operatorname{Im}(a_0 a_1^* + a_2 a_{12}^*), \quad (57)$$

$$G(\theta) = 2(|a_1|^2 + |a_{12}|^2), \quad (58)$$

$$H(\theta) = 2|b_{12}|^2, \quad (59)$$

$$K(\theta) = 2|c_{12}|^2, \quad (60)$$

$$w = \frac{2\pi}{j} \int d\varepsilon_f \delta(\varepsilon_f - \varepsilon_i) \frac{\varepsilon_f p_f}{(2\pi)^3} = \frac{\varepsilon_i^2}{(2\pi)^2}. \quad (61)$$

A similar formula for the Coulomb scattering was derived in [6,7].

Even if an unpolarized electron is scattered on an unpolarized ion, both electrons still become partially polarized. In this case, the density matrix of the initial state $\hat{\rho}_i$ reduces to the density matrix of the completely unpolarized system $\hat{\rho}_0 = \frac{1}{4}$. Using Eq. (48), we obtain the following expression for the density matrix of the two-electron system after the scattering:

$$\hat{\rho} = \frac{1}{4} MM^+. \quad (62)$$

Any 4×4 matrix can be represented in terms of the direct products of the 2×2 identity matrix I and Pauli matrices σ . It is convenient to use the following representation for the density matrix $\hat{\rho}$ since the coefficients of the expansion have clear physical meaning:

$$\hat{\rho} = \tilde{I}(\theta) \left(1 + \zeta^e(\theta) \sigma_1 + \eta^{\text{ion}}(\theta) \sigma_2 + \sum_{ij} C_{ij}(\theta) \sigma_{1i} \sigma_{2j} \right). \quad (63)$$

Here ζ^e is the polarization vector of the scattered electron, η^{ion} is the polarization vector of the ion after the scattering, and C_{ij} determines the correlation between polarizations of the electron and the ion. Using Eq. (62) and comparing it with Eqs. (50) and (54), the parameters introduced in Eq. (63) can be expressed as

$$\tilde{I}(\theta) = \frac{1}{4} \operatorname{Tr}(MM^+) = I(\theta), \quad (64)$$

$$\zeta^e = \frac{\operatorname{Tr}(MM^+ \sigma_1)}{\operatorname{Tr}(MM^+)} = \hat{\mathbf{n}} \frac{D(\theta)}{I(\theta)}, \quad (65)$$

$$\eta^{\text{ion}} = \frac{\operatorname{Tr}(MM^+ \sigma_2)}{\operatorname{Tr}(MM^+)} = \hat{\mathbf{n}} \frac{D^{\text{ion}}(\theta)}{I(\theta)}, \quad (66)$$

$$D^{\text{ion}}(\theta) = 2 \operatorname{Re}(a_0 a_2^* + a_1 a_{12}^*). \quad (67)$$

The functions D and D^{ion} determine the transverse polarization of the electron and the ion acquired in the process of scattering. The polarization vector of the scattered electron (ζ^e) can also be presented as the difference between the cross sections for scattering of an unpolarized electron on an unpolarized ion with the opposite scattered electron spin projections on $\hat{\mathbf{n}}$ ($\mu_{\perp} = \pm \frac{1}{2}$) divided by the total cross section

$$\zeta^e = \hat{\mathbf{n}} \cdot S_{0\hat{\mathbf{n}}}, \quad (68)$$

where

$$S_{\hat{\zeta}_i \hat{\zeta}_f} = \frac{\left(\frac{d\sigma}{d\Omega}\right)_{\hat{\zeta}_i \hat{\zeta}_f}^+ - \left(\frac{d\sigma}{d\Omega}\right)_{\hat{\zeta}_i \hat{\zeta}_f}^-}{\left(\frac{d\sigma}{d\Omega}\right)_{\hat{\zeta}_i \hat{\zeta}_f}^+ + \left(\frac{d\sigma}{d\Omega}\right)_{\hat{\zeta}_i \hat{\zeta}_f}^-}, \quad (69)$$

$$\left(\frac{d\sigma}{d\Omega}\right)_{\hat{\zeta}_i \hat{\zeta}_f}^{\pm} = \frac{d\sigma}{d\Omega}(\mathbf{p}_i, \hat{\zeta}_i; \mathbf{p}_f, \pm \hat{\zeta}_f). \quad (70)$$

It follows from Eq. (54) that

$$S_{0\hat{\mathbf{n}}} = S_{\hat{\mathbf{k}}\hat{\mathbf{n}}} = S_{\hat{\mathbf{q}}\hat{\mathbf{n}}} = S_{\hat{\mathbf{p}}\hat{\mathbf{n}}}, \quad (71)$$

so scattering of electrons polarized in any direction in the plane of scattering (for example, along momentum \mathbf{p}_i) can also be used to determine ζ^e .

Using Eqs. (65), (68), and (71), we can write

$$S_{0\hat{\mathbf{n}}} = S_{\hat{\mathbf{k}}\hat{\mathbf{n}}} = S_{\hat{\mathbf{q}}\hat{\mathbf{n}}} = S_{\hat{\mathbf{p}}\hat{\mathbf{n}}} = \frac{D(\theta)}{I(\theta)}. \quad (72)$$

Also, the following expressions can be derived for the remaining functions:

$$S_{\hat{\mathbf{q}}\hat{\mathbf{k}}} = -S_{\hat{\mathbf{k}}\hat{\mathbf{q}}} = \frac{F(\theta)}{I(\theta)}, \quad (73)$$

$$S_{\hat{\mathbf{n}}\hat{\mathbf{n}}} = 1 - \frac{H(\theta) + K(\theta)}{I(\theta) + D(\theta)}, \quad (74)$$

$$S_{-\hat{\mathbf{n}}-\hat{\mathbf{n}}} = 1 - \frac{H(\theta) + K(\theta)}{I(\theta) - D(\theta)}, \quad (75)$$

$$S_{\hat{\mathbf{k}}\hat{\mathbf{k}}} = 1 - \frac{G(\theta) + K(\theta)}{I(\theta)}, \quad (76)$$

$$S_{\hat{\mathbf{q}}\hat{\mathbf{q}}} = 1 - \frac{G(\theta) + H(\theta)}{I(\theta)}. \quad (77)$$

The differential cross section for the scattering of electrons with nonzero projection of polarization in the direction perpendicular to the momentum of the incident electron is dependent not only on the polar angle θ but also on the azimuthal angle φ (the direction of $\hat{\mathbf{n}}$ is defined by the plane of scattering and changes with the azimuthal angle φ corresponding to the momentum of the scattered electron):

$$\frac{d\sigma}{d\Omega}(\theta, \varphi) = \frac{1}{4} w I(\theta) \left(1 + \frac{D(\theta)}{I(\theta)} (\zeta_i \hat{\mathbf{n}}) \right). \quad (78)$$

Now consider the scattering of a polarized electron on an unpolarized ion. Similarly to Eq. (65), the polarization of the

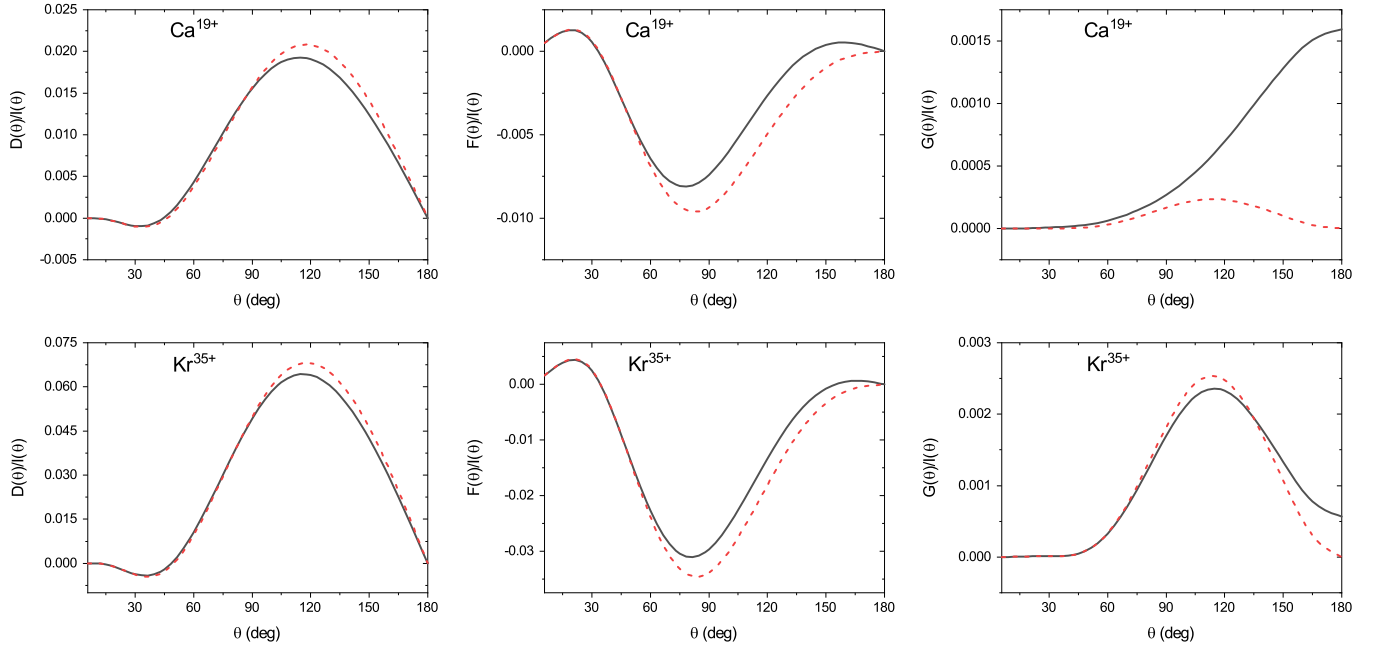


FIG. 1. Functions $D(\theta)/I(\theta)$ (left column), $F(\theta)/I(\theta)$ (middle column), and $G(\theta)/I(\theta)$ (right column) for nonresonant scattering on Ca^{19+} and Kr^{35+} (black solid line) and Coulomb scattering by the screened potential of the nucleus (red dashed line). The kinetic energy of incident electron is 2.77 keV for Ca^{19+} and 9.22 keV for Kr^{35+} .

scattered electron is given by

$$\zeta^e = \frac{\text{Tr}[M(1 + \zeta_i \sigma_1) M^+ \sigma_1]}{\text{Tr}[M(1 + \zeta_i \sigma_1) M^+]}. \quad (79)$$

For polarizations directed along \hat{n} and perpendicular to \hat{n} we get

$$\zeta_i = \pm \hat{n} \longrightarrow \zeta_{\perp}^e = \pm \hat{n} \left(1 - \frac{H + K}{I \pm D} \right) = \pm \hat{n} S_{\pm \hat{n} \pm \hat{n}}, \quad (80)$$

$$\begin{aligned} \zeta_i \hat{n} = 0 \longrightarrow \zeta_{\parallel}^e &= \frac{D}{I} \hat{n} + \left(1 - \frac{G + K}{I} \right) (\zeta_i \hat{k}) \hat{k} \\ &+ \left(1 - \frac{G + H}{I} \right) (\zeta_i \hat{q}) \hat{q} - \frac{F}{I} [\zeta_i \times \hat{n}] \\ &= S_{0\hat{n}} \hat{n} + S_{\hat{k}\hat{k}} (\zeta_i \hat{k}) \hat{k} + S_{\hat{q}\hat{q}} (\zeta_i \hat{q}) \hat{q} + S_{\hat{q}\hat{k}} [\zeta_i \times \hat{n}], \end{aligned} \quad (81)$$

respectively. The function F determines the change of polarization in the scattering plane and the functions G , H , and K describe the depolarization of the electron.

III. RESULTS AND DISCUSSION

The elastic scattering of an electron on a H-like ion can proceed via nonresonant and resonant (with the formation of intermediate autoionizing states) channels. We start our discussion by considering the nonresonant channel.

A. Nonresonant scattering

Within our approach we distinguish between two interactions contributing to the elastic electron scattering: Coulomb interaction of the incident electron with the long-range potential of the ion (which does not change the polarization of the ion) and its interaction with the $1s$ electron (which can result in the spin exchange between two electrons). We note that the

Coulomb interaction with the $1s$ electron is partially taken into account nonperturbatively, so the nucleus is considered to be partially screened by the electron.

The amplitude defined by Eqs. (8) and (47) corresponds to the Coulomb interaction with the partially screened nucleus and describes the Coulomb scattering. The Coulomb scattering of polarized electrons has been thoroughly investigated (see [1,6,7,44]). According to Eq. (65), the polarization of the scattered electron is described by the function $D(\theta)$. If an unpolarized electron is scattered by the Coulomb field of the nucleus, after scattering it has a degree of polarization $D(\theta)/I(\theta)$, which then can be observed in the double-scattering experiment by looking at the dependence on the azimuthal angle of the differential cross section for the second scattering [1,44]. The effect becomes particularly noticeable for high Z . In order to check the accuracy of our calculations for the Coulomb part of the amplitude, we compared our results for $D(\theta)/I(\theta)$ with those obtained in [8]. We found them to be in excellent agreement. A special case of Eq. (54) for the Coulomb scattering cross section [with $H(\theta) = K(\theta) = 0$] is given in [6,7].

First we consider the nonresonant energy region of the incident electron. Figure 1 shows D/I , F/I , and G/I as functions of the polar angle θ for the electron scattering on Ca^{19+} and Kr^{35+} . The incident electron kinetic energies (2.77 keV for Ca^{19+} and 9.22 keV for Kr^{35+}) are chosen so that the resonances are far enough to make no contribution. The black solid line corresponds to the scattering on the H-like ion and red dashed line represents the results of an approximation in which the role of the $1s$ electron is reduced to screening the nucleus and the exchange interaction between electrons is not taken into account. While for D/I and F/I the contribution due to the exchange interaction with the $1s$ electron is rather small and the shape of the curve is mainly determined by

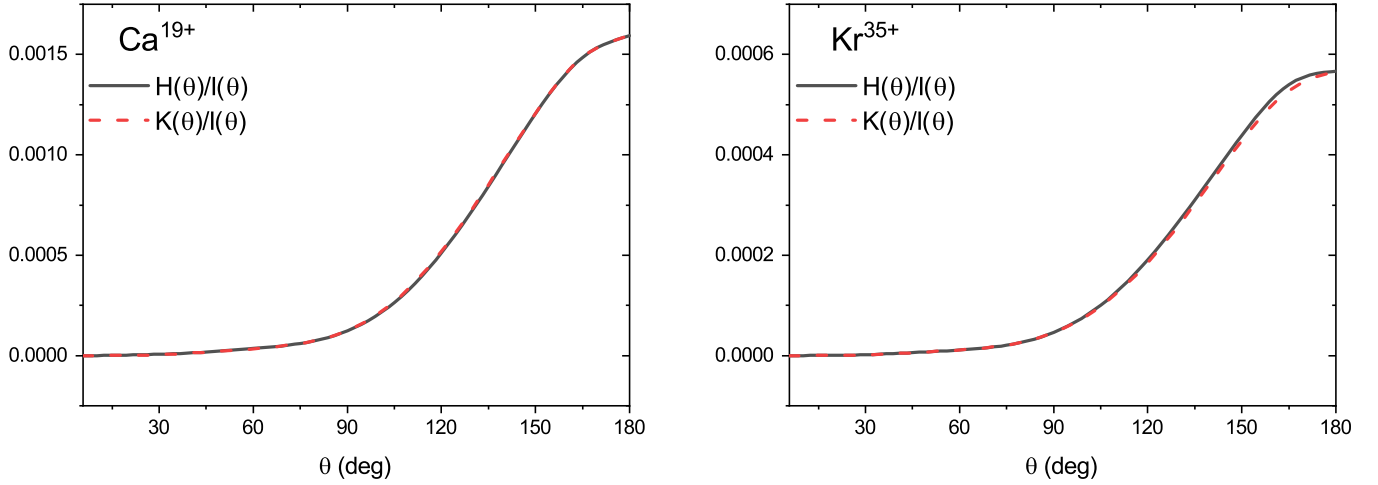


FIG. 2. Functions $H(\theta)/I(\theta)$ (black solid line) and $K(\theta)/I(\theta)$ (red dashed line) for nonresonant scattering on Ca^{19+} and Kr^{35+} . The kinetic energy of incident electron is 2.77 keV for Ca^{19+} and 9.22 keV for Kr^{35+} .

the Coulomb interaction, for G/I the situation is different. For small Z the main contribution to the function G comes from the exchange of projections of spin between the incident electron and the $1s$ electron. Thus, removing the spinor structure of the bound electron from consideration (red dashed line) leads to a significant drop in the function G . At small Z , G/I reaches a maximum at 180° . For higher Z the Coulomb scattering contribution becomes more important. The shape of the curve changes and the maximum moves to around 120° .

Figure 2 presents the functions H/I and K/I for the same energies as in Fig. 1. For the Coulomb scattering $H(\theta) = K(\theta) = 0$, which means that the electron polarization perpendicular to the plane of scattering is not changed by the scattering. In the presence of one bound electron transverse polarization change becomes possible due to the spin exchange between electrons. Since the only contribution to H/I and K/I is due to the interaction with the bound electron, these functions decrease with Z .

For the nonresonant scattering, the difference between the functions $H(\theta)$ and $K(\theta)$ is minimal (especially for small Z). Provided that $H(\theta) = K(\theta)$, we can choose $b_{12} = c_{12}$ [see Eqs. (43), (59), and (60)]. Then the matrix M defined by Eq. (43) is symmetric with respect to the rotation around \hat{n} and the directions \hat{k} and \hat{q} are no longer special. This approximate symmetry also holds for some of the resonances (see Figs. 8 and 9).

B. Resonant scattering

In the process of electron scattering by H-like ions, the energy region of the incident electron at which scattering occurs with the formation and subsequent Auger decay of autoionizing states is of particular interest. In the case of intermediate- and small- Z ions, the resonant channel becomes influential. Below we discuss that the appearance of the resonant channel leads to both qualitative and quantitative changes in the polarization parameters.

The function $D(\theta)/I(\theta)$, also known as the Sherman asymmetry function [8], determines the polarization the initially unpolarized electron acquires in the process of scattering

[Eq. (65)] as well as asymmetry with respect to the azimuthal angle φ if the scattered electron has nonzero polarization perpendicular to its momentum [Eq. (78)]. The results of our calculations of $D(\theta)/I(\theta)$ for the scattering on Ca^{19+} as a function of the incident electron kinetic energy in the vicinity of the resonances are presented in Fig. 3 for five different angles. The resonance shape strongly depends on the scattered electron angle. Depending on the resonance, $D(\theta)/I(\theta)$ reaches a maximum at $\theta = 90^\circ$ – 150° . Therefore, we chose $\theta = 120^\circ$ to study the behavior of $D(\theta)/I(\theta)$ for the scattering on different ions. The parameter D/I at $\theta = 120^\circ$ for the electron scattering on B^{4+} , Ca^{19+} , Kr^{35+} , and Xe^{53+} is presented in Fig. 4 as a function of the incident electron kinetic energy. We see that for the scattering on low- and intermediate- Z ions the formation of autoionizing states can cause a significant increase of the spin asymmetry (up to 60% for scattering on B^{4+}), which is otherwise very small (up to 2% for scattering on Ca^{19+} and even less for lighter ions). With the growth of Z , the role of the background becomes more significant.

In Figs. 5 and 6 the results for $F(\theta)/I(\theta)$ are presented in the same manner. The physical meaning of the function F/I is as follows. If the incident electron is

TABLE I. Order of resonances in Figs. 4–11.

Resonance number	Intermediate autoionizing state
1	$(2s)_0^2$
2	$(2s2p_{1/2})_1$
3	$(2s2p_{1/2})_0$
4	$(2s2p_{3/2})_2$
5	$(2p_{1/2})_0^2$
6	$(2p_{3/2})_2^2$
7	$(2p_{1/2}2p_{3/2})_1$
8	$(2p_{1/2}2p_{3/2})_2$
9	$(2s2p_{3/2})_1$
10	$(2p_{3/2})_0^2$

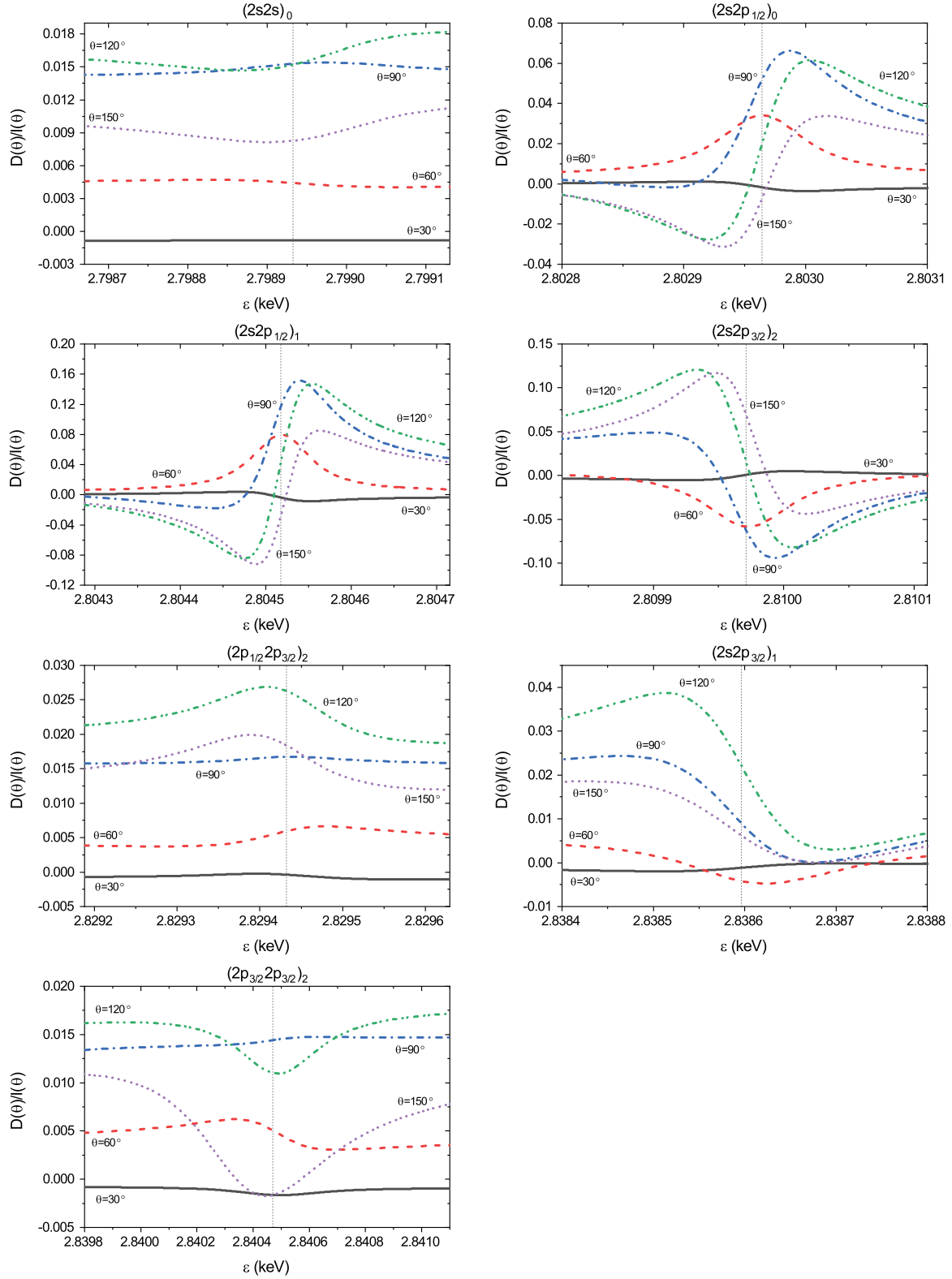


FIG. 3. Function $D(\theta)/I(\theta)$ for electron scattering on Ca^{19+} near the resonances for five different angles θ of the scattered electron. The vertical gray dashed line denotes the resonance energy.

longitudinally polarized, $F(\theta)/I(\theta)$ determines the scattered electron polarization component lying in the plane of scattering and perpendicular to the incident electron momentum.

For the description of depolarization of an electron in the process of scattering, it is convenient to alternate between the functions $G(\theta)/I(\theta)$, $H(\theta)/I(\theta)$, and $K(\theta)/I(\theta)$ [Eqs. (58)–(60)] and parameters $S_{\hat{k}\hat{k}}$, $S_{\hat{q}\hat{q}}$, and $S_{\hat{n}\hat{n}}$. The parameters $S_{\hat{\zeta}\hat{\zeta}}$

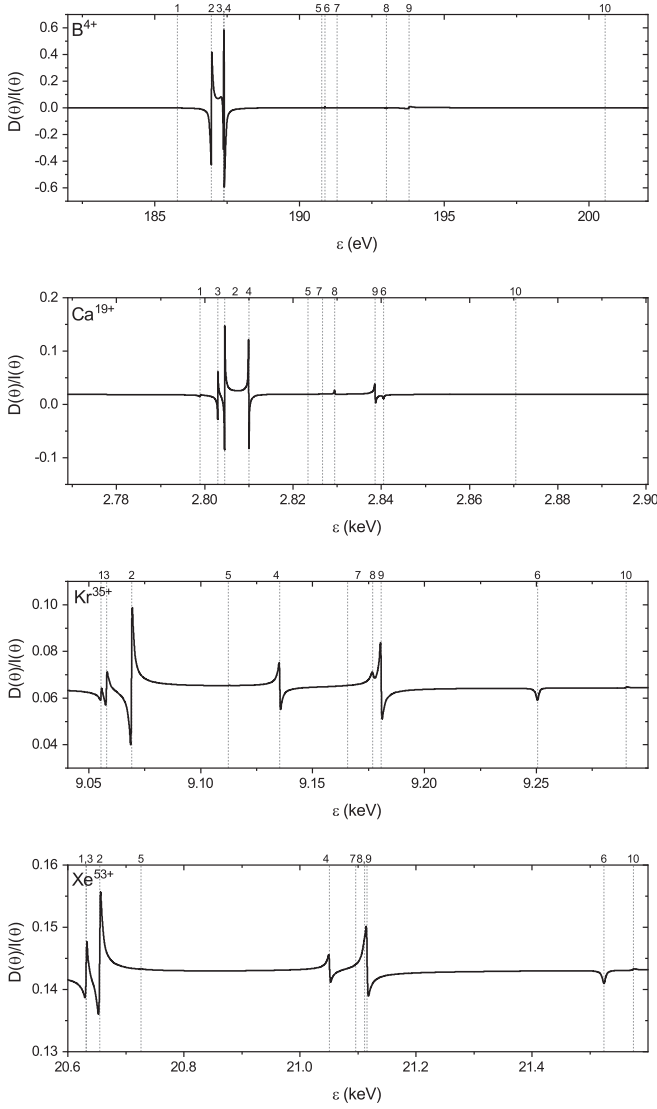


FIG. 4. Function D/I for scattering of electrons on B^{4+} , Ca^{19+} , Kr^{35+} and Xe^{53+} to the angle $\theta = 120^\circ$. The vertical dashed lines mark the positions of resonances. The corresponding autoionizing states are presented in Table I.

describe the scattering of an electron with $+\frac{1}{2}$ spin projection in the direction $\hat{\zeta}$ and represent the difference between the number of electrons that have the spin projections $+\frac{1}{2}$ and $-\frac{1}{2}$ in the direction $\hat{\zeta}$ after scattering normalized by the total number of scattered electrons [Eqs. (69) and (70)]. The parameters $S_{\hat{k}\hat{k}}$, $S_{\hat{q}\hat{q}}$, and $S_{\hat{n}\hat{n}}$ directly correspond to the change of projection of spin in a certain direction for three special directions, while the functions $G(\theta)/I(\theta)$, $H(\theta)/I(\theta)$, and $K(\theta)/I(\theta)$ have a clear connection to the coefficients b_{12} and c_{12} from Eq. (43). The connection between $G(\theta)/I(\theta)$, $H(\theta)/I(\theta)$, and $K(\theta)/I(\theta)$ and depolarization tensor introduced in [20] is presented in Appendix B.

Figures 7, 8, and 9 present the functions $G(\theta)/I(\theta)$, $H(\theta)/I(\theta)$, and $K(\theta)/I(\theta)$, respectively, for energies close to the resonances and for five different scattered electron angles. For most resonances the maxima of these functions are reached at $\theta = 180^\circ$.

Figures 10 and 11 present $S_{\hat{k}\hat{k}}(180^\circ)$ and $S_{\hat{q}\hat{q}}(180^\circ)$, respectively, for scattering on B^{4+} , Ca^{19+} , Kr^{35+} , and Xe^{53+} . We note that for the backward scattering, \hat{k} is zero for elastic scattering and \hat{n} is not well defined. The parameters $S_{\hat{k}\hat{k}}$ and $S_{\hat{n}\hat{n}}$ still exist in the limit $\theta \rightarrow \infty$ and $S_{\hat{k}\hat{k}}(180^\circ) = S_{\hat{n}\hat{n}}(180^\circ)$. These figures show that the probability of a change in the spin projection is highly dependent on the specific resonance. Since the depolarization of the electron in the direction \hat{n} is determined solely by the spin exchange, the significant deviation of the parameter $S_{\hat{n}\hat{n}}$ from unity indicates the presence of a strong exchange interaction between incident and bound electrons. While the depolarization of an electron in the plane of scattering can occur in the absence of spin exchange due to the spin-orbit interaction, in the case of the elastic scattering on H-like ions the corresponding parameters $S_{\hat{k}\hat{k}}$ and $S_{\hat{q}\hat{q}}$ are heavily influenced by the exchange interaction.

Figure 12 shows the depolarization asymmetry for the scattering of electrons on B^{4+} with opposite polarizations along \hat{n} . The asymmetry manifests in the difference between $S_{\hat{n}\hat{n}}$ and $S_{-\hat{n}-\hat{n}}$. The incident electron energy and the scattering angle were chosen to maximize the asymmetry function D/I . Again, we see that the asymmetry is significant in the resonance region.

C. Change of ionic polarization

In the collisions of an unpolarized electron with an unpolarized ion the ion also acquires polarization perpendicular to the plane of scattering equal to $D^{\text{ion}}(\theta)/I(\theta)$. Figure 13 presents the function $D^{\text{ion}}(\theta)/I(\theta)$ for the electron scattering on B^{4+} as a function of the incident electron kinetic energy (on the left) and as a function of the scattered electron angle (on the right).

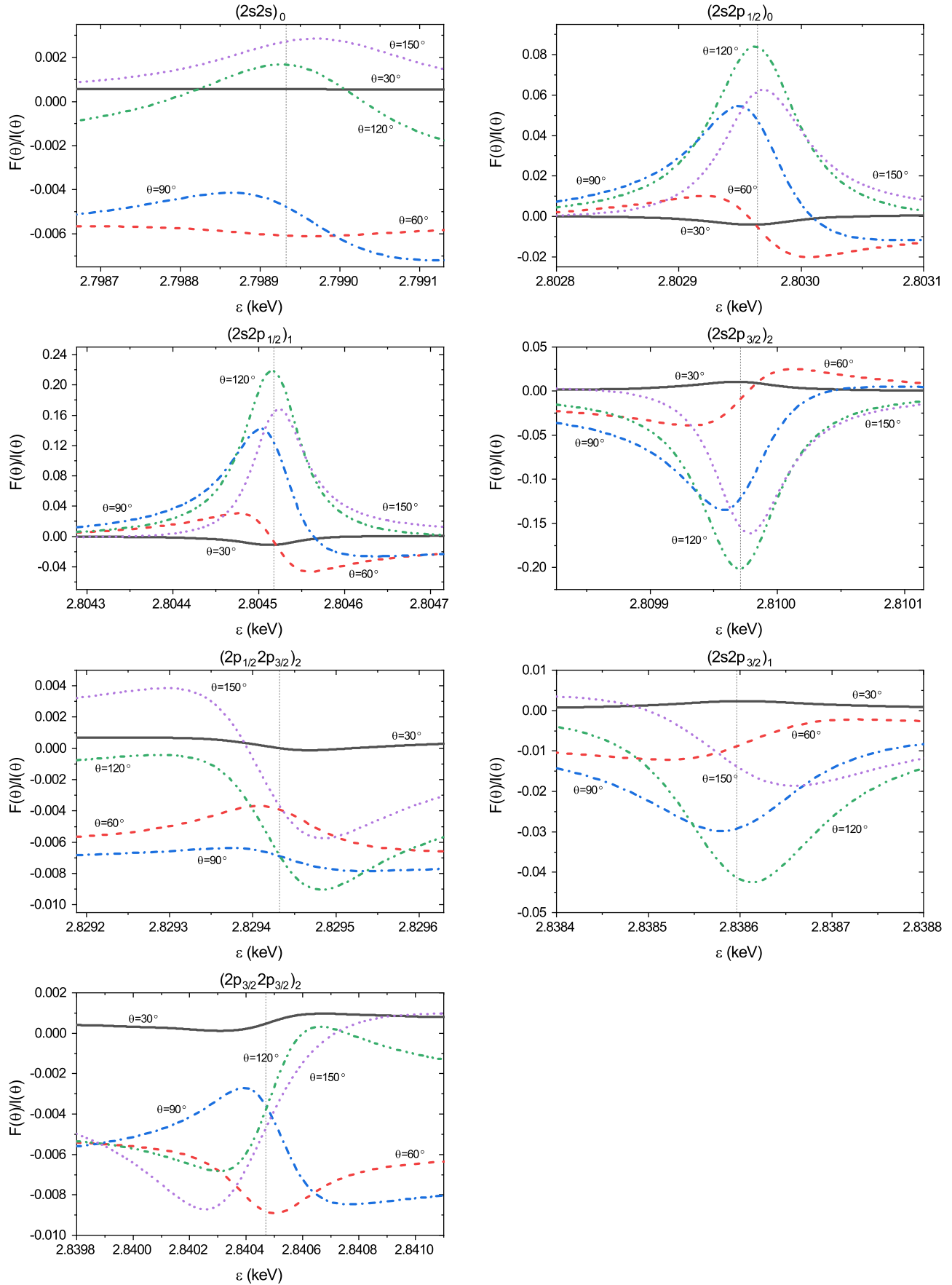
This parameter determines the polarization that an initially unpolarized ion acquires in the process of scattering as well as the asymmetry of the differential cross section for the scattering on polarized ions. It is the analog of the Sherman asymmetry function for ions. We found that for B^{4+} the asymmetry is significant and for certain impact energies and scattering angles it can reach 70%. As in the case of electrons, this asymmetry can be used for producing or measuring ion polarization.

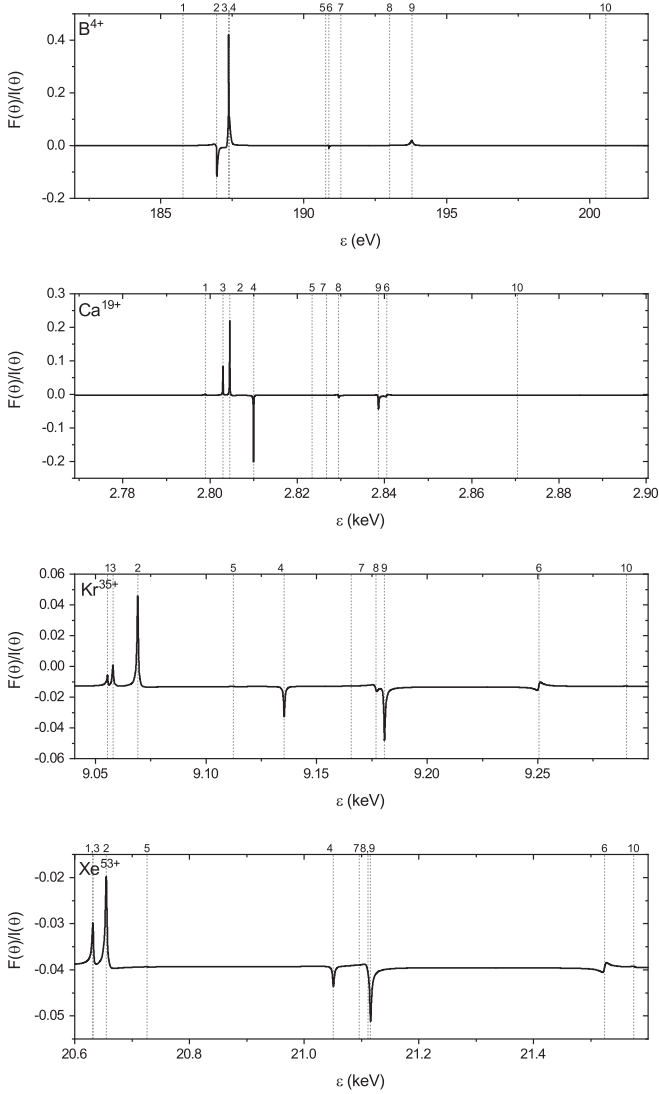
The function $D^{\text{ion}}(\theta)/I(\theta)$ also determines the cross-section asymmetry with respect to the azimuthal angle φ . If an unpolarized electron is scattered from a polarized ion, the differential cross section is dependent on both polar and azimuthal angles. If the polarization of the ion η is given by the degree of polarization P , the polar angle χ , and the azimuthal angle ω , the cross section can be written as

$$\frac{d\sigma}{d\Omega}(\theta, \varphi) \sim I(\theta) + D^{\text{ion}}(\theta)P \sin \chi \sin(\omega - \varphi). \quad (82)$$

This formula is completely analogous to Eq. (78) with ζ and $D(\theta)$ switched to η and $D^{\text{ion}}(\theta)$.

We note that polarized ion beams can be used for tests of fundamental symmetries [45–47]. However, at present the production of polarized beams of highly charged ions as well as the control and measurement of the polarization is a challenge for experimentalists [47,48]. The asymmetry of the cross section caused by the polarization of the ion beam, given


 FIG. 5. Same as in Fig. 3 but for $F(\theta)/I(\theta)$.

FIG. 6. Same as in Fig. 4 but for F/I .

by Eq. (82), can be used to measure the ion beam polarization. By looking at the asymmetry of the cross section with respect to φ one can determine the ion polarization component transverse to the incident electron momentum. If θ is fixed then the maximum and the minimum of the differential cross sections are reached at $\varphi = \omega - \pi/2$ and $\varphi = \omega + \pi/2$, respectively, and the difference between the maximum and the minimum is equal to $2D^{\text{ion}}(\theta)P_{\perp}$, where P_{\perp} is the ion polarization component transverse to the incident electron momentum. A similar principle is used in Mott polarimetry [3]. In the case of resonant electron scattering, the asymmetry increases significantly and its measurement can be used to determine the polarization of the beams of highly charged ions.

IV. CONCLUSION

We have presented a detailed study of the polarization properties of the elastic electron scattering on H-like ions. Our study was carried out within the framework of the relativistic QED theory, which is perfectly suited to describe both the spin-orbit and exchange interactions determining the change

of polarization in this process. We have considered the scattering on a wide range of ions (from B^{4+} to Xe^{53+}), paying special attention to impact energies at which intermediate LL-shell autoionizing states are formed. We have explicitly shown that the involvement of the autoionization states leads to quantitative and qualitative changes in the polarization parameters, in particular, significantly increasing the spin asymmetry. In our case the effect of autoionizing states turned out to be much stronger than that reported in [20] for the electron scattering on a neutral atom.

We have also demonstrated that for the resonant electron scattering on ions with Z up to 50, not only the relativistic spin-orbit but also the exchange interaction plays a crucial role and, as a result, the polarization properties are determined by their joint action. In particular, the exchange interaction, by enabling spin transfer between the incident and bound electrons, can fundamentally change the polarization of the scattered electron.

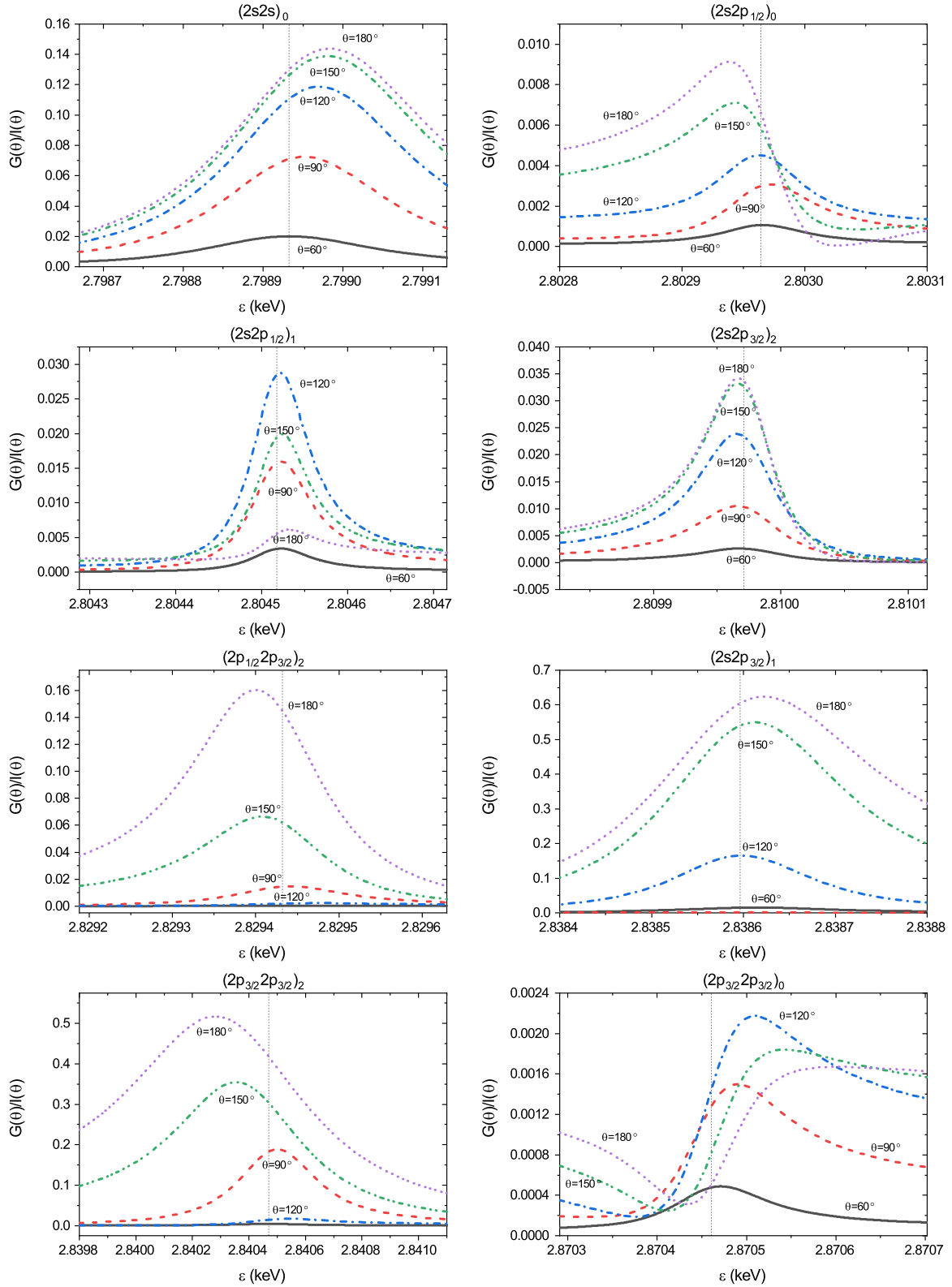
Our main focus was on the scattering of electrons on unpolarized ions. The electron polarization change in this process can be completely described by the five parameters D , F , G , H , and K together with the unpolarized differential cross section I [see Eqs. (31)–(37)]. These five parameters were calculated and thoroughly investigated for both the nonresonant and resonant energy regions as functions of the incident electron energy and the scattered electron angle. Unlike previous studies, our method allows us to accurately account for the possible spin exchange between the incident electron and the ion and to investigate the behavior of parameters G , H , and K , which are heavily influenced by the spin exchange. In fact, the parameters H and K become nonzero only when the spin-exchange interaction is taken into account.

We have shown that, unlike the case of electron potential scattering on light ions (where the unpolarized incident electron essentially does not acquire polarization), in the process of resonant scattering on unpolarized light ions the initially unpolarized electron can gain very significant polarization (up to 60% for B^{4+} ions). In turn, the ion also acquires significant polarization.

We have also considered the elastic scattering of unpolarized electrons by polarized ions. The nonzero polarization of the ion beam leads to the asymmetry of the differential cross section with respect to the rotation around the incident electron momentum. The fact that this asymmetry increases significantly in the resonance region can be used to measure the polarization of low- and intermediate- Z highly charged H-like ions.

ACKNOWLEDGMENTS

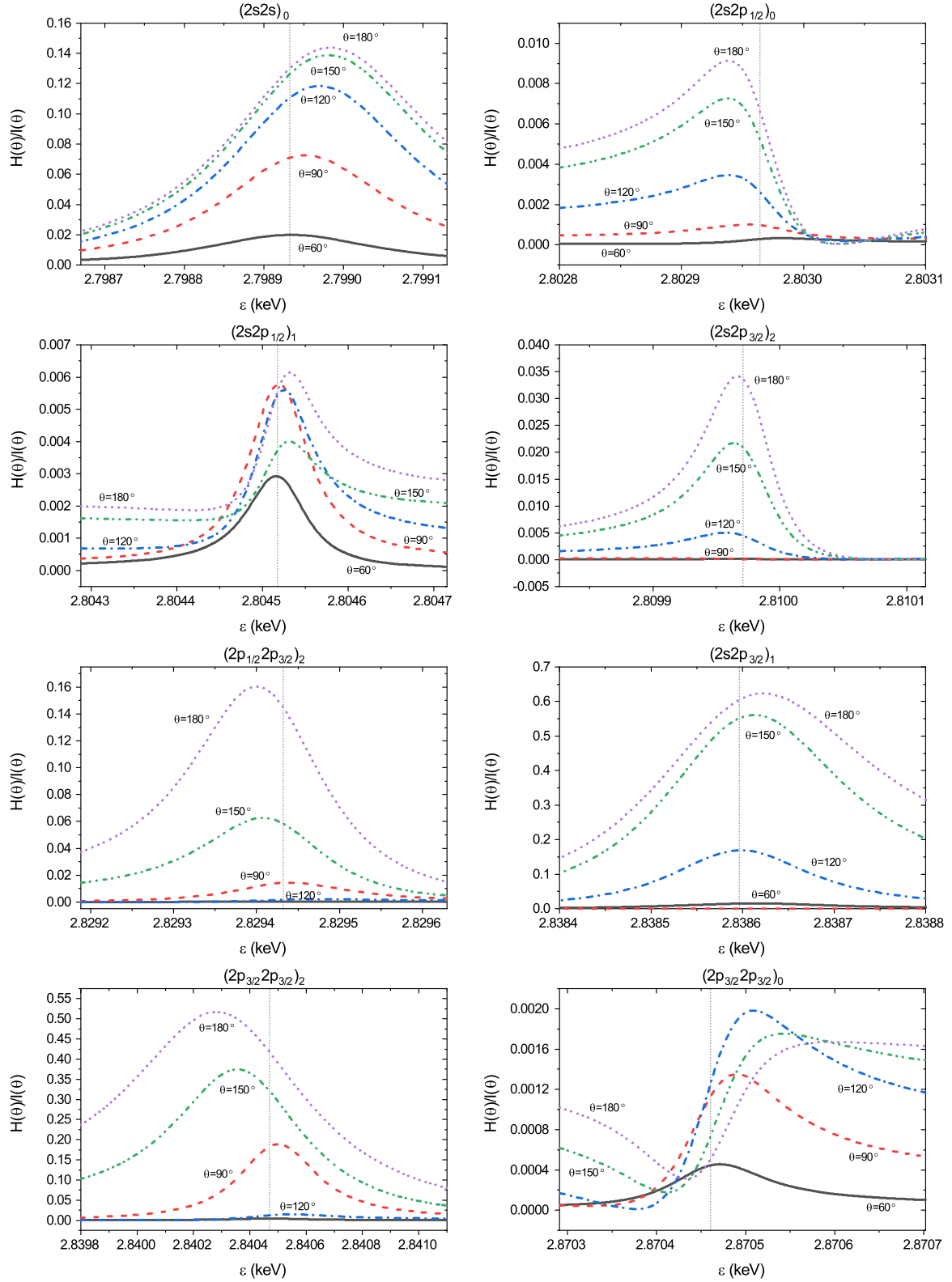
The work of D.M.V. was supported by the Dmitri Mendeleev program (Grant No. FPI 57516244). The work of D.M.V. and O.Y.A. on the calculation of the differential cross section was supported solely by the Russian Science Foundation under Grant No. 17-12-01035. The reported study was funded by RFBR and NSFC according to the Project No. 20-52-53028. This work was supported by the National Key Research and Development Program of China under Grant No. 2017YFA0402300, the National Natural Science Foundation of China under Grant No. 11774356,


 FIG. 7. Same as in Fig. 3 but for $G(\theta)/I(\theta)$.

the Chinese Academy of Sciences President's International Fellowship Initiative under Grant No. 2018VMB0016, and Chinese Postdoctoral Science Foundation under Grant No. 2020M673538.

APPENDIX A

For the sake of convenience, we choose the indices of the matrix M to be in the order $(++, +-, -+, --)$, where the first index refers to the polarization μ and the second index

FIG. 8. Same as in Fig. 3 but for $H(\theta)/I(\theta)$.

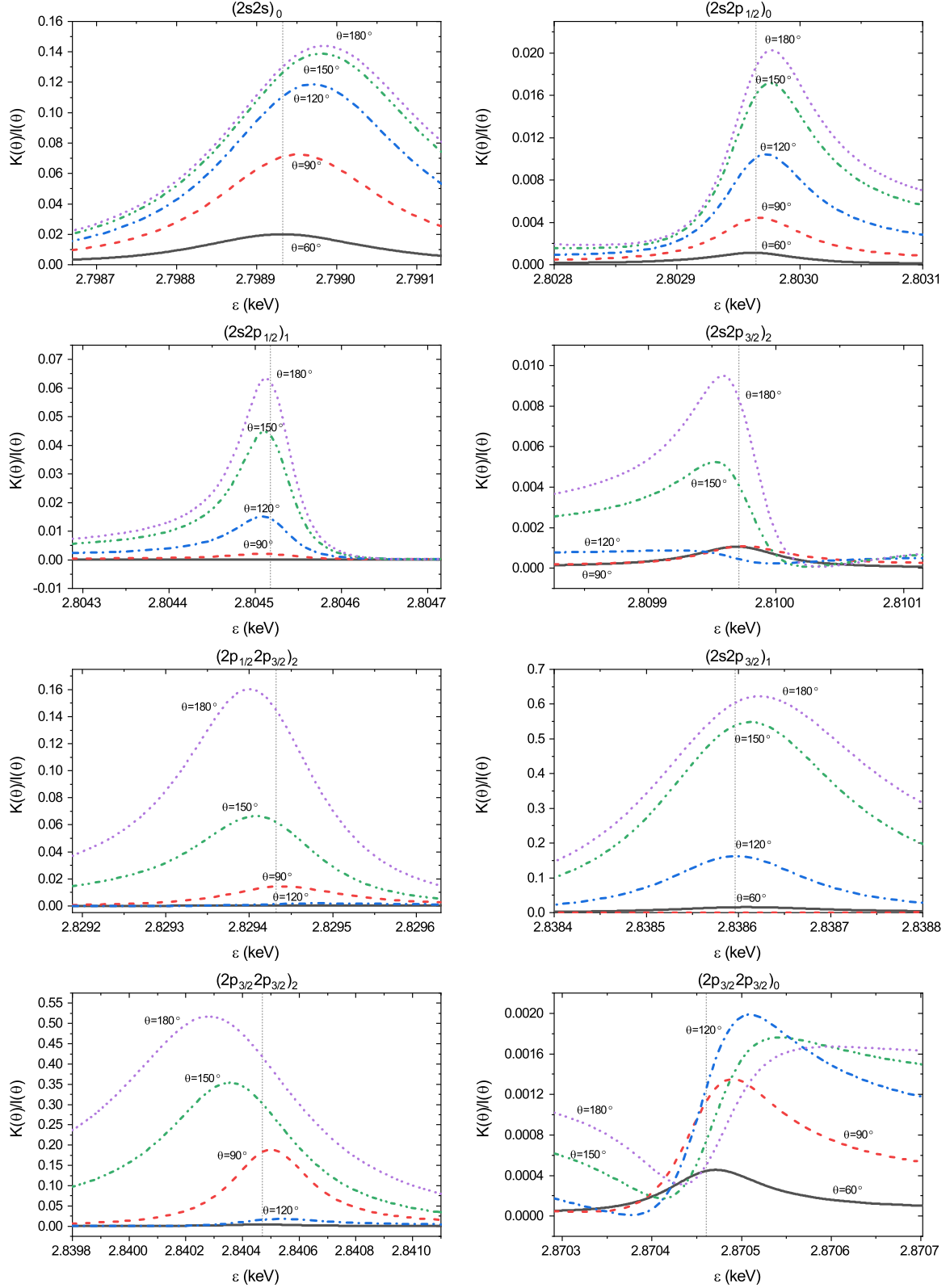
refers to the spin projection to the z axis m of the bound electron. Also, we set the initial polarization μ_i equal to $+1/2$. Then the corresponding eight matrix elements can be written as

$$M_{11} = U_{m_i=+1/2, \mu_i=+1/2; m_f=+1/2, \mu_f=+1/2}, \quad (\text{A1})$$

$$M_{21} = U_{m_i=+1/2, \mu_i=+1/2; m_f=-1/2, \mu_f=+1/2}, \quad (\text{A2})$$

$$M_{31} = U_{m_i=+1/2, \mu_i=+1/2; m_f=+1/2, \mu_f=-1/2}, \quad (\text{A3})$$

$$M_{41} = U_{m_i=+1/2, \mu_i=+1/2; m_f=-1/2, \mu_f=-1/2}, \quad (\text{A4})$$


 FIG. 9. Same as in Fig. 3 but for $K(\theta)/I(\theta)$.

$$M_{12} = U_{m_i=-1/2, \mu_i=+1/2; m_f=+1/2, \mu_f=+1/2}, \quad (\text{A5})$$

$$M_{32} = U_{m_i=-1/2, \mu_i=+1/2; m_f=+1/2, \mu_f=-1/2}, \quad (\text{A7})$$

$$M_{22} = U_{m_i=-1/2, \mu_i=+1/2; m_f=-1/2, \mu_f=+1/2}, \quad (\text{A6})$$

$$M_{42} = U_{m_i=-1/2, \mu_i=+1/2; m_f=-1/2, \mu_f=-1/2}. \quad (\text{A8})$$

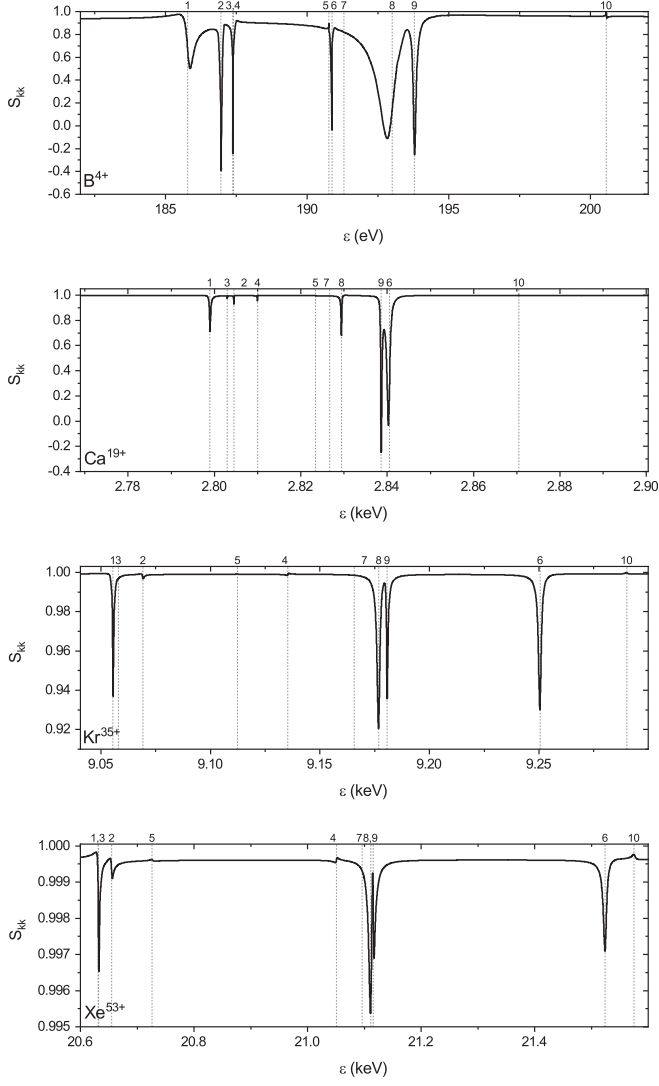


FIG. 10. Parameter S_{kk} for scattering of electrons on B^{4+} , Ca^{19+} , Kr^{35+} , and Xe^{53+} to the angle $\theta = 180^\circ$. For the backward scattering $S_{\hat{n}\hat{n}}$ coincides with S_{kk} . The vertical dashed lines mark the positions of resonances. The corresponding autoionizing states are presented in Table I.

If these matrix elements are known, the remaining eight can be easily found since

$$U_{m_i, \mu_i; m_f, \mu_f} = U_{-m_i, -\mu_i; -m_f, -\mu_f} e^{2i(m_i + \mu_i - m_f - \mu_f)\varphi} (-1)^{m_i + \mu_i - m_f - \mu_f}. \quad (A9)$$

Then for the coefficients in the expansion of M [Eq. (43)] we can write

$$a_0 = \frac{M_{11} + M_{22}}{2}, \quad (A10)$$

$$a_1 = \frac{M_{31} + M_{42}}{2i} e^{-i\varphi}, \quad (A11)$$

$$a_2 = \frac{M_{21} e^{-i\varphi} - M_{12} e^{i\varphi}}{2i}, \quad (A12)$$

$$a_{12} = \frac{M_{32} - M_{41} e^{-2i\varphi}}{2}, \quad (A13)$$

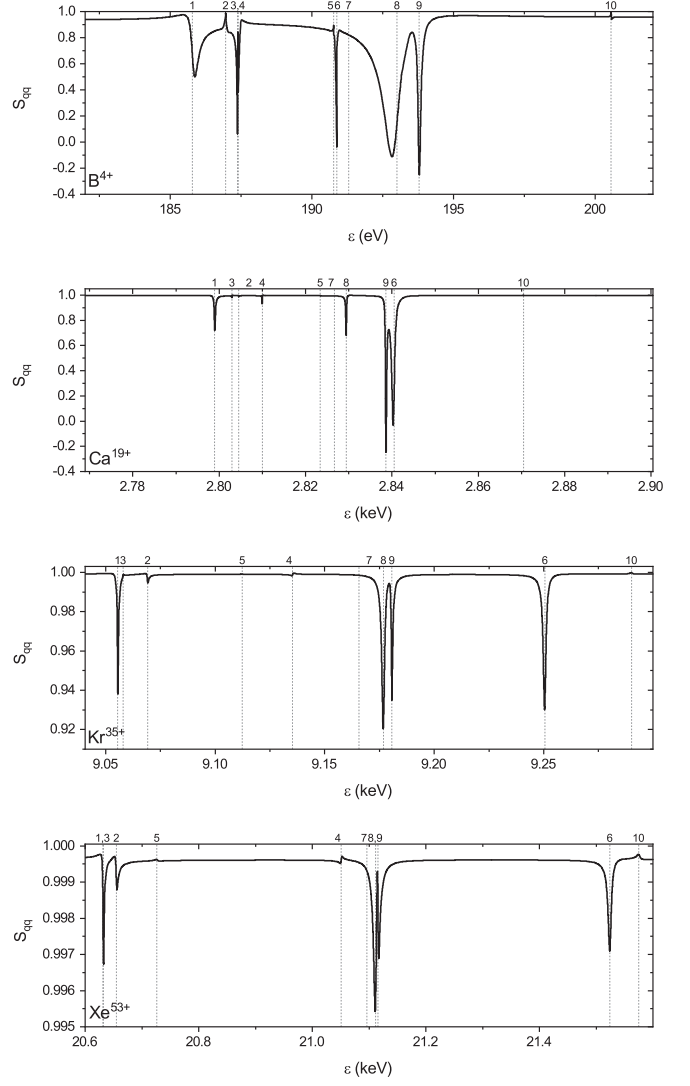


FIG. 11. Same as in Fig. 4 but for $S_{\hat{q}\hat{q}}$.

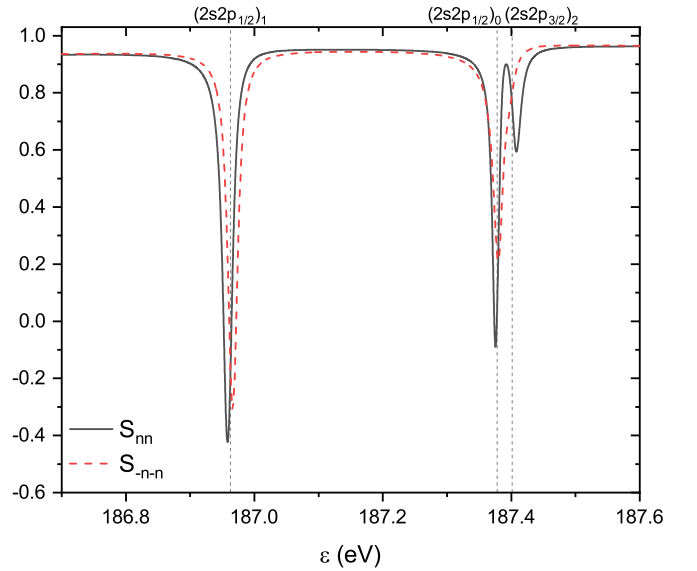


FIG. 12. Parameters $S_{\hat{n}\hat{n}}$ (black solid line) and $S_{-\hat{n}-\hat{n}}$ (red dashed line) for scattering on B^{4+} to the angle $\theta = 120^\circ$ in the vicinity of $(2s2p_{1/2})_1$, $(2s2p_{1/2})_0$, and $(2s2p_{3/2})_2$ resonances.

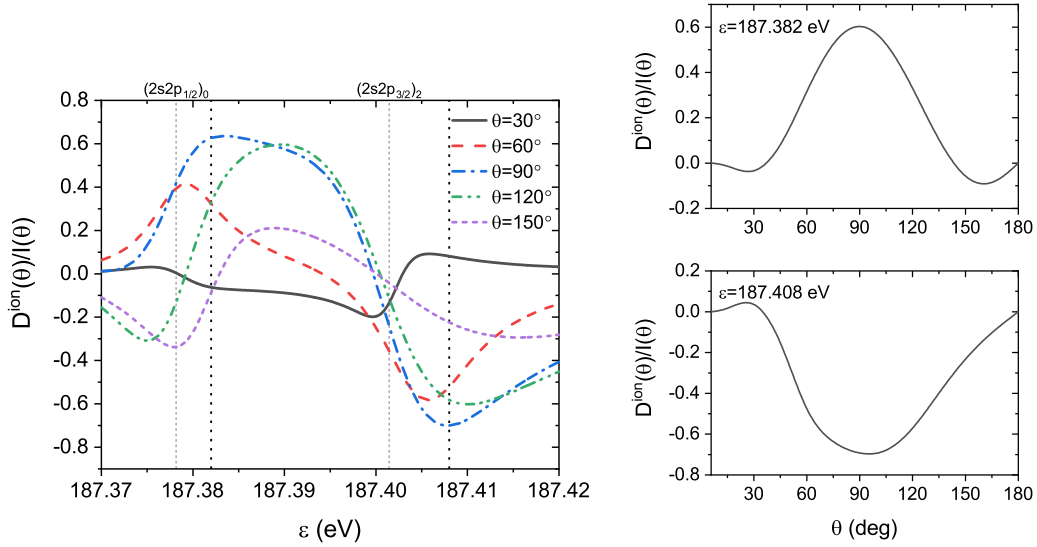


FIG. 13. Plot of $D^{\text{ion}}(\theta)/I(\theta)$ for scattering on B^{4+} as a function of incident electron energy ϵ in the vicinity of $(2s2p_{1/2})_0$ and $(2s2p_{3/2})_2$ resonances (graph on the left) and as a function of θ at energies marked by black dotted lines on the left graph (graphs on the right).

$$b_{12} = (1 + \sec \theta) \frac{M_{11} - M_{22}}{4} + (1 - \sec \theta) \frac{M_{41}e^{-2i\varphi} + M_{32}}{4} \quad (\text{A14})$$

$$= \frac{M_{11} - M_{22}}{2} + \tan \frac{\theta}{2} \frac{M_{21}e^{-i\varphi} + M_{12}e^{i\varphi}}{2}, \quad (\text{A15})$$

$$c_{12} = (1 - \sec \theta) \frac{M_{11} - M_{22}}{4} + (1 + \sec \theta) \frac{M_{41}e^{-2i\varphi} + M_{32}}{4} \quad (\text{A16})$$

$$= \frac{M_{11} - M_{22}}{2} - \cot \frac{\theta}{2} \frac{M_{21}e^{-i\varphi} + M_{12}e^{i\varphi}}{2}. \quad (\text{A17})$$

Also, since M can be described with six complex numbers, out of the eight matrix elements defined above only six are independent:

$$M_{42} - M_{31} + M_{21} + M_{12}e^{2i\varphi} = 0, \quad (\text{A18})$$

$$\begin{aligned} \sin \theta (M_{11} - M_{22} - M_{32} - M_{41}e^{-2i\varphi}) \\ - 2 \cos \theta (M_{21}e^{-i\varphi} + M_{12}e^{i\varphi}) = 0. \end{aligned} \quad (\text{A19})$$

The additional symmetry at $\theta = \pi$ results in additional limitations on the functions D , F , G , and H at this angle. Consider backward scattering ($\theta = \pi$ and $\hat{p}_i = \hat{q}$). If the incident electron is polarized along the direction of its momentum, the process is symmetric with respect to the z axis, which means that the cross section does not depend on the electron polarization perpendicular to the z axis. Therefore, $S_{\hat{p},\hat{n}} = S_{\hat{p},\hat{k}} = 0$ and $S_{\hat{n}\hat{n}} = S_{\hat{k}\hat{k}}$. This, along with Eqs. (69), (70), and (72)–(77), immediately leads to

$$D(\pi) = 0, \quad F(\pi) = 0, \quad G(\pi) = H(\pi). \quad (\text{A20})$$

APPENDIX B

In previous investigations of the electron scattering a number of parameters were introduced to characterize the

polarization properties. In this paper we adapted the set of parameters used to describe the Coulomb scattering in [7] to the electron scattering on H-like ions. The following formulas can be used to switch to the notation introduced by Burke for the electron scattering on H-like ions [20]:

$$I_0 = I, \quad (\text{B1})$$

$$P = \frac{D}{I}, \quad (\text{B2})$$

$$D_{kq} = \frac{F}{I}, \quad (\text{B3})$$

$$D_{nn} = 1 - \frac{H + K}{I}, \quad (\text{B4})$$

$$D_{kk} = 1 - \frac{G + K}{I}, \quad (\text{B5})$$

$$D_{qq} = 1 - \frac{G + H}{I}. \quad (\text{B6})$$

In order to describe the polarization properties of the electron scattering on atoms, the parameters S , T , and U are usually introduced [18]. While for the resonant electron scattering on H-like ions the use of only three parameters is clearly insufficient, we can still establish the connection between S , T , and U and the parameters introduced in this paper. If we neglect the spin exchange between the incident and bound electrons, the parameters $H(\theta)$ and $K(\theta)$ become zero. In that case,

$$S(\theta) = \frac{D(\theta)}{I(\theta)}, \quad (\text{B7})$$

$$T(\theta) = 1 - \frac{G(\theta)}{I(\theta)}, \quad (\text{B8})$$

$$U(\theta) = \frac{F(\theta)}{I(\theta)}, \quad (\text{B9})$$

and

$$S^2 + T^2 + U^2 = 1. \quad (\text{B10})$$

- [1] N. F. Mott, *Proc. R. Soc. London Ser. A* **124**, 425 (1929).
- [2] C. G. Shull, C. T. Chase, and F. E. Myers, *Phys. Rev.* **63**, 29 (1943).
- [3] T. J. Gay and F. B. Dunning, *Rev. Sci. Instrum.* **63**, 1635 (1992).
- [4] X. Roca-Maza, *Europhys. Lett.* **120**, 33002 (2017).
- [5] F. Lipps and H. Tolhoek, *Physica* **20**, 85 (1954).
- [6] H. A. Tolhoek, *Rev. Mod. Phys.* **28**, 277 (1956).
- [7] W. R. Johnson, T. A. Weber, and C. J. Mullin, *Phys. Rev.* **121**, 933 (1961).
- [8] N. Sherman, *Phys. Rev.* **103**, 1601 (1956).
- [9] S.-R. Lin, N. Sherman, and J. K. Percus, *Nucl. Phys.* **45**, 492 (1963).
- [10] H. L. Cox and R. A. Bonham, *J. Chem. Phys.* **47**, 2599 (1967).
- [11] A. Gellrich and J. Kessler, *Phys. Rev. A* **43**, 204 (1991).
- [12] M. Dummmler, G. F. Hanne, and J. Kessler, *J. Phys. B* **28**, 2985 (1995).
- [13] A. Dorn, A. Elliott, J. Lower, S. F. Mazevet, R. P. McEachran, I. E. McCarthy, and E. Weigold, *J. Phys. B* **31**, 547 (1998).
- [14] F. Salvat, A. Jablonski, and C. Powell, *Comput. Phys. Commun.* **165**, 157 (2005).
- [15] A. K. F. Haque, M. M. Haque, P. P. Bhattacharjee, M. A. Uddin, M. A. R. Patoary, M. I. Hossain, A. K. Basak, M. S. Mahbub, M. Maaza, and B. C. Saha, *J. Phys. Commun.* **1**, 035014 (2017).
- [16] D. Jakubassa-Amundsen, *Nucl. Phys. A* **975**, 107 (2018).
- [17] M. Dragowski, M. Włodarczyk, G. Weber, J. Ciborowski, J. Enders, Y. Fritzsche, and A. Poliszczuk, *Nucl. Instrum. Methods Phys. Res. Sect. B* **389–390**, 48 (2016).
- [18] M. Dapor, *Sci. Rep.* **8**, 5370 (2018).
- [19] M. Kokkoris, A. Lagoyannis, and F. Maragkos, *Nucl. Instrum. Methods Phys. Res. Sect. B* **461**, 44 (2019).
- [20] P. G. Burke and J. F. B. Mitchell, *J. Phys. B* **7**, 214 (1974).
- [21] S. Ait-Tahar, I. P. Grant, and P. H. Norrington, *Phys. Rev. Lett.* **79**, 2955 (1997).
- [22] K. Bartschat and Y. Fang, *Phys. Rev. A* **62**, 052719 (2000).
- [23] G. Baum, N. Pavlovic, B. Roth, K. Bartschat, Y. Fang, and I. Bray, *Phys. Rev. A* **66**, 022705 (2002).
- [24] M. F. Ahmed, W. Ji, R. P. McEachran, and A. D. Stauffer, *J. Phys. B* **40**, 4119 (2007).
- [25] R. K. Gangwar, A. N. Tripathi, L. Sharma, and R. Srivastava, *J. Phys. B* **43**, 085205 (2010).
- [26] C. J. Bostock, D. V. Fursa, and I. Bray, *Phys. Rev. A* **86**, 062701 (2012).
- [27] C. J. Bostock, D. V. Fursa, and I. Bray, *J. Phys. B* **45**, 181001 (2012).
- [28] B. A. Huber, C. Ristori, C. Guet, D. Küchler, and W. R. Johnson, *Phys. Rev. Lett.* **73**, 2301 (1994).
- [29] J. B. Greenwood, I. D. Williams, and P. McGuinness, *Phys. Rev. Lett.* **75**, 1062 (1995).
- [30] G. Toth, S. Grabbe, P. Richard, and C. P. Bhalla, *Phys. Rev. A* **54**, R4613 (1996).
- [31] T. J. M. Zouros, E. P. Benis, and T. W. Gorczyca, *Phys. Rev. A* **68**, 010701(R) (2003).
- [32] E. P. Benis, T. J. M. Zouros, T. W. Gorczyca, A. D. González, and P. Richard, *Phys. Rev. A* **69**, 052718 (2004).
- [33] E. P. Benis, T. J. M. Zouros, T. W. Gorczyca, A. D. González, and P. Richard, *Phys. Rev. A* **73**, 029901(E) (2006).
- [34] K. N. Lyashchenko, D. M. Vasileva, O. Y. Andreev, and A. B. Voitkiv, *Phys. Rev. Research* **2**, 013087 (2020).
- [35] A. I. Akhiezer and V. B. Berestetskii, *Quantum Electrodynamics* (Wiley Interscience, New York, 1965).
- [36] P. G. Burke, *R-Matrix Theory of Atomic Collisions* (Springer-Verlag, Berlin, 2011).
- [37] O. Y. Andreev, L. N. Labzowsky, G. Plunien, and D. A. Solov'yev, *Phys. Rep.* **455**, 135 (2008).
- [38] P. J. Mohr, G. Plunien, and G. Soff, *Phys. Rep.* **293**, 227 (1998).
- [39] N. J. Snyderman, *Ann. Phys. (NY)* **211**, 43 (1991).
- [40] V. A. Yerokhin and V. M. Shabaev, *Phys. Rev. A* **60**, 800 (1999).
- [41] V. M. Shabaev, *Phys. Rep.* **356**, 119 (2002).
- [42] O. Y. Andreev, L. N. Labzowsky, and A. V. Prigorovskiy, *Phys. Rev. A* **80**, 042514 (2009).
- [43] J. Kessler, *Polarized Electrons* (Springer, Berlin, 1985).
- [44] N. F. Mott, *Proc. R. Soc. London Ser. A* **135**, 429 (1932).
- [45] I. Khriplovich, *Phys. Lett. B* **444**, 98 (1998).
- [46] I. Khriplovich, *Hyperfine Interact.* **127**, 365 (2000).
- [47] A. Bondarevskaya, A. Prozorov, L. Labzowsky, G. Plunien, D. Liesen, and F. Bosch, *Phys. Rep.* **507**, 1 (2011).
- [48] A. Surzhykov, S. Fritzsche, T. Stöhlker, and S. Tashenov, *Phys. Rev. Lett.* **94**, 203202 (2005).